CR-132514

THE CHEMISTRY AND DIFFUSION OF AIRCRAFT EXHAUSTS IN THE LOWER STRATOSPHERE DURING THE FIRST FEW HOURS AFTER FLY-BY

Glenn R. Hilst

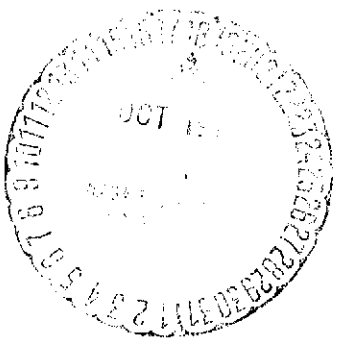

Prepared under Contract NAS1-12475 by
Aeronautical Research Associates of Princeton, Inc.
50 Washington Road, Princeton, New Jersey 08540

for

NATIONAL AERONAUTICS AND SPACE ADMINISTRATION

July 1974

A.R.A.P. Report No. 216 CR-132514

THE CHEMISTRY AND DIFFUSION OF AIRCRAFT EXHAUSTS IN THE LOWER STRATOSPHERE DURING THE FIRST FEW HOURS AFTER FLY-BY

Glenn R. Hilst

Prepared under Contract NAS1-12475 by
Aeronautical Research Associates of Princeton, Inc.
50 Washington Road, Princeton, New Jersey 08540

for

NATIONAL AERONAUTICS AND SPACE ADMINISTRATION

July 1974

THE CHEMISTRY AND DIFFUSION OF AIRCRAFT EXHAUSTS IN THE LOWER STRATOSPHERE DURING THE FIRST FEW HOURS AFTER FLY-BY

Glenn R. Hilst

Aeronautical Research Associates of Princeton, Inc.

SUMMARY

In support of the U. S. Department of Transportation's Climatic Impact Assessment Program, the Aeronautical Research Associates of Princeton have undertaken an analysis of the hydrogen-nitrogen-oxygen reaction systems in the lower stratosphere as these are perturbed initially by individual aircraft engine exhaust plumes. These analyses were directed primarily to the question, "Do any significant chemical reactions occur either among exhaust chemical species or between these species (and their products) and the environmental ozone while the exhaust products are confined in intact plume segments at relatively high concentrations?" Secondarily, the joint effects of diffusive mixing and chemical kinetics on these reactions were investigated, using the techniques of second-order closure diffusion/chemistry models developed by Donaldson (ref. 1) and Hilst (ref. 2) at A.R.A.P. Operated in a coupled mode, these models permit quantitative assessments of the effects of inhomogeneous mixing and diffusion limitations on the chemical reaction rates.

Throughout these studies attention has been focussed on the larger problem of the potential depletion of ozone by SST exhaust materials emitted into the lower stratosphere. Although the analyses completed to date are handicapped by inadequate observational data, needed both as input to the models and for validation of the predictions, the following results have emerged:

- Under a variety of conditions of aircraft emissions of NO and H_2O and of aircraft-induced and natural turbulence, the depletion of O_3 in the early post-vortex plume remains as a critical variable in the immediate post-vortex chemistry. Within reasonable emission rates of NO, a significant "O_3-hole" is possible.

• Only under what appears to be 1) rather extreme concentrations of water vapor and/or photolysis rates, and 2) minimum emissions of NO, is there a significant conversion of NO_x to HNO_3 during the first few sunlit hours after fly-by. This conclusion could be tempered by more exact data on H_2O emissions, stratospheric turbulence, and photolysis rates, but, insofar as present estimates are reliable, early HNO_3 formation cannot be depended upon for subsequent buffering of the NO_x catalytic cycle for O_3 destruction.

INTRODUCTION

During the past two years, the Aeronautical Research Associates of Princeton have undertaken analyses of SST-related chemistry and diffusion in support of the DOT/CIAP studies. This work was carried on under Contracts NAS1-11433, NAS1-11873 and NAS1-12475. This report constitutes the final report on NAS1-12475, and has also been prepared for publication, in a somewhat amended form, in fulfillment of NAS1-11873.

The present report is one small part of the analyses which the U. S. Department of Transportation's Climatic Impact Assessment Program (CIAP) and a world-wide community of scientists are assembling. It is also a very specialized study, directed to the processes of chemical reactions and turbulent diffusion in individual SST exhaust plumes during the first few hours of their existence. Prior to the CIAP analyses this phase of the overall problem was generally ignored, although it was clear that the genesis of any environmental problems must be the individual aircraft's contribution. In particular, during the first few hours or days of their existence these exhaust products can be expected to be confined to relatively intact plume segments at concentrations much in excess of their background levels in the lower stratosphere. (We have termed this phase the "highly perturbed stratosphere.") Noting this fact, the question arises, "Does anything significant happen during this period of high concentrations?"

The next logical question, of course, is, "Can anything significant happen?" Several possibilities worth exploring come to mind. For example, given the very stable temperature structure of the lower stratosphere, the exhaust materials may be confined in these plume segments for extended periods of time, periods during which they are not in chemical contact with the environmental constituents with which they may react, such as ozone. If this is the case, the local environmental impact of the exhaust materials could be severe, but these volumes could also be such a minute fraction of the total stratosphere that such effects would be totally negligible.

As another example, chemical reactions which convert environmentally hazardous exhaust constituents into relatively inert materials can proceed at a much more rapid rate when high concentrations obtain. A prime example, which is explored in depth here, is the conversion of NO to NO_2 and thence to HNO_3 in the presence of sunlight, O_3, and H_2O. This complex process, which would effectively buffer the NO_x catalytic cycle for the destruction of O_3, is particularly effective when the concentration of H_2O is well above background stratospheric levels. However, this process also depends upon an adequate amount of O_3, which must be supplied by either local chemical production or by turbulent entrainment of the neighboring environmental O_3. In order to assess this possibility we must, therefore, work with coupled chemistry and diffusion simulation systems.

As the reader may judge for himself from what follows, these studies of the chemistry and diffusion of the highly perturbed stratosphere suggest that there may be important chemical processes which go on during the early life of individual SST plumes. However, the question as to whether or not these processes actually do occur cannot be answered now. Much harder data on the small-scale turbulence in the stratosphere and a critical testing of the chemical chains assumed in these analyses, particularly as they actually occur in the stratosphere are required. Happily, analyses such as the present one point the way to obtaining this critical information.

THE PROBLEMS POSED

A qualitative description of the pertinent features of an SST engine exhaust plume during the first few hours after a single SST has flown by in the lower stratosphere provides the framework for the quantitative treatment of the diffusion and chemistry of the exhaust materials and environmental constituents which follows. First, it is important to recognize that the lower stratosphere (15-22 km above mean sea level) is characterized by generally strong hydrostatic stability. As a result, local wind shear-produced turbulence is practically nonexistent (ref. 2). Larger-scale meandering wind currents, and some vertical wind velocity variations are observed, but the production of small-scale turbulence capable of mixing individual SST exhaust plumes with the ambient atmosphere appears to depend upon occasional breaking waves arising from either external perturbations, e.g., mountain waves, or unstable internal gravity waves. As a result, it can be assumed that small-scale turbulence in the lower stratosphere is both sporadic, rather than continuous, and of relatively short duration. Aircraft observations (ref. 3) suggest detectable levels of small-scale turbulence occur only one to five per cent of the time, and individual turbulence "bursts" persist for only a few minutes to an hour or so.

If this general picture of turbulence, on the scale necessary to diffuse the initial SST exhaust plume, is approximately correct, we should expect that a very large fraction of these plumes will be emitted into an atmosphere which is in essentially laminar flow conditions. However, there is one important source of small-scale turbulence which must be considered, namely, the turbulence induced by the passage of the aircraft itself, particularly the decay of the wing-tip vortices. The sequence of events which this turbulence produces is shown in Fig. 1. Unfortunately, the quantitative treatment of the vortex roll-up, the onset of instability, and the structure and decay of small-scale turbulence during the five to ten minutes it takes for these events to occur is not yet available. In this part of the problem we must still settle for largely qualitative and empirical estimates. The importance of this simple fact, and the need to acquire a considerably improved resolution of this phase of the problem, resides in the chemistry which goes on during this brief but critical time, and in the specification of the concentration distributions of critical exhaust components as they enter the post-vortex phase of their existence (Fig. 1).

From the viewpoint of the subsequent effects of NO_x and H_2O on the environmental O_3, we are particularly interested in the entrainment of O_3 and the conversion of NO to NO_2 during the vortex decay phase. During the vortex phase, the SST exhaust plume is characterized by concentrations of NO and H_2O which are orders of magnitude above ambient values. However, during the vortex roll-up phase these plumes are also essentially O_3- and NO_2-free. O_3, of course, is relatively abundant in the environment surrounding the plume, but, until vortex breakup occurs, there is no guaranteed source of turbulence to mix the NO and O_3. If this mixing is initiated and sustained for a few minutes, a highly significant chain of chemical reactions is initiated:

1. O_3 reacts with NO to produce NO_2 and O_2.
2. In the sunlit sky, photodissociation of NO_2 and O_3 produces $O(^3P)$ and $O(^1D)$, as well as NO and O_2.
3. $O(^3P)$ reacts with O_2 and M to form O_3.
4. $O(^1D)$ reacts with H_2O to form 2 OH radicals.
5. OH reacts with NO_2 to form HNO_3.

Other reactions occur as well, but this sequence, occurring as it does at greatly elevated concentrations of NO_x and H_2O, poses the possibility that a significant fraction of the NO is converted to HNO_3 during the first few hours of the plume's existence. Given the inert character of HNO_3, so far as O_3 is concerned, and its slow photodissociation back to NO_2 and OH, this conversion, if realized, strongly buffers the NO_x catalytic cycle for the destruction of O_3.

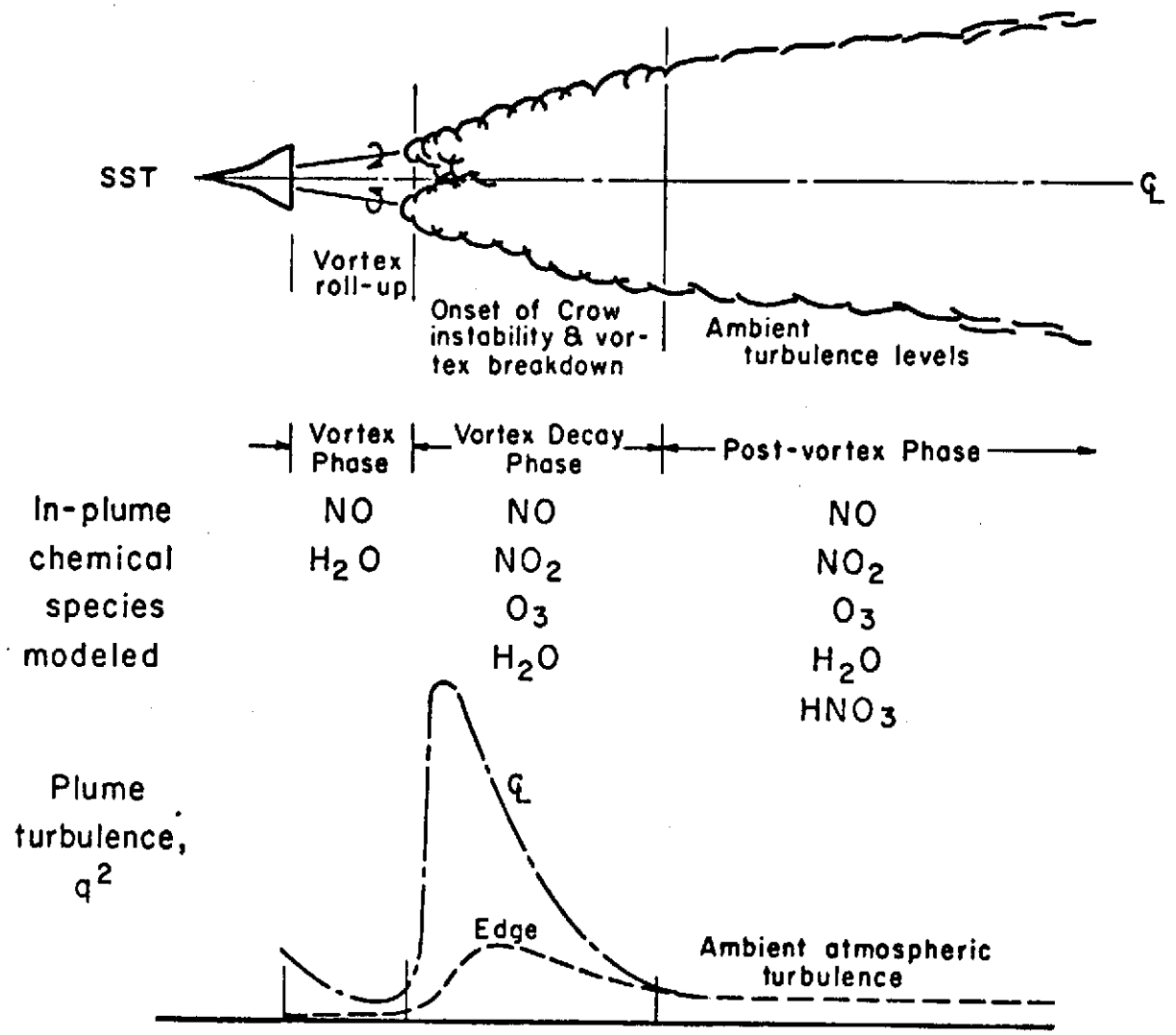

Figure 1. A qualitative description of the early history of individual SST engine exhaust plumes, the turbulence fields, and the critical chemical species involved in determining the fate of O_3 and NO_x during this time.

When and if this is the case is a major problem considered here. For now, however, it is important to realize that this whole sequence depends critically upon the conversion of NO to NO_2 in the plume while the concentrations of NO_x and H_2O are still large. This sequence must be initiated by the entrainment of environmental O_3, a process which necessarily leads to the dilution of the plume-bound NO_x and H_2O. Clearly, we have a potentially fine balance between diffusion and kinetic processes in a system which is characterized by inhomogeneous mixing.

Against this background, the Aeronautical Research Associates of Princeton (A.R.A.P.) has undertaken an evolutionary program of model development and analyses in support of the CIAP objectives. The initial problems addressed were directed primarily to the rate at which individual SST plumes would spread until they achieved lateral dimensions of the order of the large-scale (global) models' grid spacing. (During this time global models cannot resolve individual plume features.) Coupled with this diffusion study, we have examined the problem of relatively simple chemistry between exhaust and environmental constituents, and to what degree these reactions might be limited by either inadequate turbulent mixing or by inhomogeneous mixing. The results of these early studies have been reported (refs. 2 and 4) and are not repeated here.

In the latter stages of this study we have focussed attention on the problems associated with combined chemistry and diffusion in individual SST plumes during the time they exist in high concentrations and in relatively intact plume segments. Attention has been directed first to the problems of interactions between the oxides of nitrogen, NO and NO_2, and O_3 and the impact of turbulent mixing on these processes. The results of this study have been reported by Hilst (ref. 5).

As a result of the NO_x-O_3 study, it was concluded that the possibility of a significant conversion of NO and NO_2 to HNO_3 during the early plume history deserved a detailed analysis. This problem constitutes the final phase of this study for CIAP and, since it subsumes all of the earlier analyses, it is the primary topic of this report. In addressing this latter problem, it is, of course, necessary to include the water vapor component of the SST exhaust. This makes it possible to address the important problem of the comparative roles of H_2O and NO_x in determining the O_3 balance in the stratosphere.

THE ANALYTICAL TOOLS

Based on the earlier work of Donaldson (refs.6, 7) and Donaldson and Hilst (ref. 8), it was evident that the techniques of second-order closure of the equations for turbulent dynamics and chemical kinetics, using the principles of invariance postulated by Donaldson, were particularly applicable to the problems of early SST plume behavior. In fact, the problem of inhomogeneous mixing and its effect on fast chemical reaction rates required an ability to handle the prediction of the dynamic behavior of second-order correlations of concentration fluctuations in turbulent mixing. These correlations could be expected to be strongly time dependent, and not subject to simple parameterization by mean value characteristics of the flow, plume shape, and chemical reaction rates. An analysis of the possible limits of the effects of incomplete mixing by Hilst (ref. 2) showed this could be a significant feature of early SST plume behavior, but deferred the identification of when or under what circumstances this is the case to full model calculations.

Beyond this requirement for dynamic models which explicitly include the second-order moments, it was also recognized that the invariant models provide a ready check on the circumstances under which first-order closure models provide an adequate representation of the combined chemistry and diffusion processes. These model predictions, and the parameters associated with them, such as effective diffusivity, are recovered explicitly as limiting cases of the second-order closure model predictions (cf. Donaldson (ref. 1)). The exercising of the invariant model for the SST plume conditions also served the useful purpose of "tuning up" the first-order closure models used by others. These results have been summarized by Hilst (ref. 9).

The detailed development of invariant models for the prediction of turbulence and turbulent diffusion in shear flows has been reported by Donaldson (ref. 1); the development of an invariant model for the chemical kinetics of binary, isothermal reactions and the coupling of these kinetic models with the diffusion models have been reported by Hilst (refs. 2, 5). Briefly, these modeling techniques, which date back to Keller and Friedman (ref. 10) but were implicit in the work of Reynolds (ref. 11), take advantage of the fact that the dynamical equation for the behavior of two jointly fluctuating variables, say x' and y', can be written

$$\frac{\partial x'y'}{\partial t} = x' \frac{\partial y'}{\partial t} + y' \frac{\partial x'}{\partial t} \qquad (1)$$

For example, and as an illustration of the second-order closure technique, consider the chemical kinetics of an isothermal binary reaction specified by

$$\alpha + \beta \xrightarrow{k} \gamma + \delta \tag{2}$$

Then

$$\frac{\partial[\alpha]}{\partial t} = - k[\alpha][\beta] \tag{3}$$

and

$$\frac{\partial[\beta]}{\partial t} = - k[\alpha][\beta] \tag{4}$$

where [i] denotes the local concentration of the ith chemical species, and k is the appropriate reaction rate constant. For convenience of notation let $x = [\alpha]$ and $y = [\beta]$, and we assume ensemble averages of x and y can be formed such that

$$x = \overline{x} + x' \tag{5}$$

and

$$y = \overline{y} + y' \tag{6}$$

where $\overline{x'} = \overline{y'} \equiv 0$.

But

$$\frac{\partial x'}{\partial t} = \frac{\partial x}{\partial t} - \frac{\partial \overline{x}}{\partial t} \tag{7}$$

$$\frac{\partial y'}{\partial t} = \frac{\partial y}{\partial t} - \frac{\partial \overline{y}}{\partial t} \tag{8}$$

From Eqs. (3)-(6)

$$\frac{\partial \overline{x}}{\partial t} + \frac{\partial x}{\partial t} = - k(\overline{x}\,\overline{y} + \overline{x}\,y' + \overline{y}\,x' + x'y') \tag{9}$$

and

$$\frac{\partial \overline{y}}{\partial t} + \frac{\partial y}{\partial t} = - k(\overline{x}\,\overline{y} + \overline{x}\,y' + \overline{y}\,x' + x'y') \tag{10}$$

Taking the ensemble averages of Eqs. (9) and (10)

$$\frac{\partial \overline{x}}{\partial t} = - k(\overline{x}\,\overline{y} + \overline{x'y'}) \tag{11}$$

and

$$\frac{\partial \bar{y}}{\partial t} = - k(\bar{x}\ \bar{y} + \overline{x'y'}) \tag{12}$$

Subtracting (11) from (9) and (12) from (10) gives

$$\frac{\partial x'}{\partial t} = - k(\bar{x}\ y' + \bar{y}\ x' + x'y' - \overline{x'y'}) \tag{13}$$

and

$$\frac{\partial y'}{\partial t} = - k(\bar{x}\ y' + \bar{y}\ x' + x'y' - \overline{x'y'}) \tag{14}$$

Multiplying (13) and (14) by y' and x', respectively,

$$y' \frac{\partial x'}{\partial t} = - k(\bar{x}\ y'^2 + \bar{y}\ x'y' + x'y'^2 - y'\overline{x'y'}) \tag{15}$$

and

$$x' \frac{\partial y'}{\partial t} = - k(\bar{x}\ x'y' + \bar{y}\ x'^2 + x'^2y' - x'\overline{x'y'} \tag{16}$$

Adding (15) and (16) and again taking an ensemble average,

$$\frac{\partial \overline{x'y'}}{\partial t} = - k(\bar{x}\ \overline{y'^2} + \bar{y}\ \overline{x'y'} + \overline{x'y'^2})$$

$$- k(\bar{x}\ \overline{x'y'} + \bar{y}\ \overline{x'^2} + \overline{x'^2y'}) \tag{17}$$

Equation (17) introduces four new variables, $\overline{x'^2}$, $\overline{y'^2}$, $\overline{x'^2y'}$, and $\overline{x'y'^2}$, for which prediction equations are required. The first two are readily obtained by multiplying (13) and (14) by $2x'$ and $2y'$ respectively, and averaging

$$\frac{\partial \overline{x'^2}}{\partial t} = - 2k(\bar{x}\ \overline{x'y'} + \bar{y}\ \overline{x'^2} + \overline{x'^2y'}) \tag{18}$$

and

$$\frac{\partial \overline{y'^2}}{\partial t} = - 2k(\bar{x}\ \overline{y'^2} + \bar{y}\ \overline{x'y'} + \overline{x'y'^2}) \tag{19}$$

At this stage, the chemical kinetics model is

$$\frac{\partial \overline{x}}{\partial t} = - k(\overline{x}\ \overline{y} + \overline{x'y'}) \tag{20}$$

$$\frac{\partial \overline{y}}{\partial t} = - k(\overline{x}\ \overline{y} + \overline{x'y'}) \tag{21}$$

$$\frac{\partial \overline{x'y'}}{\partial t} = - k(\overline{x}\ \overline{y'^2} + \overline{y}\ \overline{x'y'} + \overline{x'y'^2}$$

$$- k(\overline{x}\ \overline{x'y'} + \overline{y}\ \overline{x'^2} + \overline{x'^2y'}) \tag{22}$$

$$\frac{\partial \overline{x'^2}}{\partial t} = - 2k(\overline{x}\ \overline{x'y'} + \overline{y}\ \overline{x'^2} + \overline{x'^2y'}) \tag{23}$$

and

$$\frac{\partial \overline{y'^2}}{\partial t} = - 2k(\overline{x}\ \overline{y'^2} + \overline{y}\ \overline{x'y'} + \overline{x'y'^2}) \tag{24}$$

a set of five simultaneous partial differential equations involving seven unknowns. If we choose to "close" the system at this level, we are obliged to find expressions for $\overline{x'^2y'}$ and $\overline{x'y'^2}$ in terms of $\overline{x}$, $\overline{y}$, $\overline{x'y'}$, $\overline{x'^2}$, and $\overline{y'^2}$. Since the first and second moments of x and y cannot generally contain all of the information necessary to specify $\overline{x'^2y'}$ and $\overline{x'y'^2}$, these expressions are necessarily approximate, a situation which is generally true at any level of closure.

We seek these approximate relationships from the general definition of a third-order moment, i.e.,

$$\overline{x'^2y'} = \frac{1}{N} \sum_{i=1}^{N} n_i(\overline{x} + x_i')^2(\overline{y} + y_i') \tag{25}$$

Expanding the right-hand side of (25), rearranging terms, and dividing by $\overline{x}^2\overline{y}$ gives

$$\frac{\overline{x'^2y'}}{\bar{x}^2\,\bar{y}} = -\left(1 + 2\,\frac{\overline{x'y'}}{\bar{x}\,\bar{y}} + \frac{\overline{x'^2}}{\bar{x}^2}\right)$$

$$+ \frac{1}{\bar{x}^2\,\bar{y}\,N}\sum_{i=1}^{N} n_i x_i^2 y_i \qquad (26)$$

(The definition of $\overline{x'y'^2}$ is obtained by simply interchanging x and y in (26).) We note immediately from Eq. (26) that the explicit information regarding the third-order moments contained in the first- and second-order moments can be identified by the bracketed term on the right-hand side, and the problem is reduced to finding a useful approximation for the summation term in Eq. (26). This term is, of course, the third-order moment of the joint frequency distribution $n_i(x_i,y_i)$ about the origin of the (x,y) plane.

From the general properties of $n_i(x_i, y_i)$, we can immediately deduce the following conditions which Eq. (26) must satisfy:

1. When either x' or y' ≡ 0,

$$\frac{1}{\bar{x}^2\,\bar{y}\,N}\sum_{i=1}^{N} n_i x_i^2 y_i = 1$$

2. When n_i is nonzero only for $(0, y_i)$ and $(x_i, 0)$,

$$\frac{1}{\bar{x}^2\,\bar{y}\,N}\sum_{i=1}^{N} n_i x_i^2 y_i = 0 \text{ and } \overline{x'y'} = -\bar{x}\,\bar{y}$$

Then

$$\frac{1}{\bar{x}^2\,\bar{y}\,N}\sum_{i=1}^{N} n_i x_i^2 y_i = \frac{\overline{x'^2y'}}{\bar{x}^2\,\bar{y}} + \frac{\overline{x'^2}}{\bar{x}^2} - 1$$

(This is the condition for termination of the reaction due to local depletion of either of the reacting chemical species.)

3. When $\overline{x'y'} = 0$ (random distributions of x_i and y_i)

$$\frac{1}{\bar{x}^2\,\bar{y}\,N}\sum_{i=1}^{N} n_i x_i^2 y_i = \frac{\overline{x'^2 y'}}{\bar{x}^2\,\bar{y}} + \frac{\overline{x'^2}}{\bar{x}^2} + 1$$

4. When $\overline{x'^2 y'} = 0$

$$\frac{1}{\bar{x}^2\,\bar{y}\,N}\sum_{i=1}^{N} n_i x_i^2 y_i = 1 + 2\,\frac{\overline{x'y'}}{\bar{x}\,\bar{y}} + \frac{\overline{x'^2}}{\bar{x}^2}$$

These four conditions should be satisfied by any approximate model of $\overline{x'^2 y'}$.

A useful model of $\overline{x'^2 y'}$ and $\overline{x' y'^2}$, developed out of these considerations at A.R.A.P. (ref. 2), is

$$\overline{x'^2 y'} = \frac{\bar{x}^2\,\bar{y}}{M+1}\left[1 + \frac{\overline{x'^2}}{\bar{x}^2} + 2\,\frac{\overline{x'y'}}{\bar{x}\,\bar{y}}\right]\left[\frac{\overline{x'y'}}{\bar{x}\,\bar{y}} - M\right] \qquad (27)$$

and

$$\overline{x' y'^2} = \frac{\bar{x}\,\bar{y}^2}{M+1}\left[1 + \frac{\overline{y'^2}}{\bar{y}^2} + 2\,\frac{\overline{x'y'}}{\bar{x}\,\bar{y}}\right]\left[\frac{\overline{x'y'}}{\bar{x}\,\bar{y}} - M\right] \qquad (28)$$

where M is either 0 or 1 according to whether

$$\left(\frac{\overline{x'^2}}{\bar{x}^2}\,\frac{\overline{y'^2}}{\bar{y}^2}\right) \lessgtr 1 \qquad (29)$$

The importance of retaining the higher-order moments in the chemical kinetics model is demonstrated for the case when x_i and y_i are jointly log-normally distributed with an initial value of $\overline{x'^2}\;\overline{y'^2}/\bar{x}^2\,\bar{y}^2 = 8100$. The predicted reaction rates, $\partial\bar{x}/\partial t$, for three cases, 1) mean-value chemistry, i.e., $\overline{x'} = \overline{y'} = 0$, 2) when only $\overline{x'y'}$, $\overline{x'^2}$, and $\overline{y'^2}$ are retained, i.e., $\overline{x'^2 y'} = \overline{x' y'^2} \equiv 0$, and 3) the full A.R.A.P. chemical model, are compared with the exact solution of the chemical kinetics equations in Fig. 2. The neglect of all fluctuations grossly underestimates the reaction rate; neglect of the third-order moments results in a large overestimate of this rate; and inclusion of these terms as modeled here captures almost exactly the time history of the reaction rate for this situation. It should also be noted that as $\overline{x'^2}/\bar{x}^2$ and $\overline{y'^2}/\bar{y}^2$

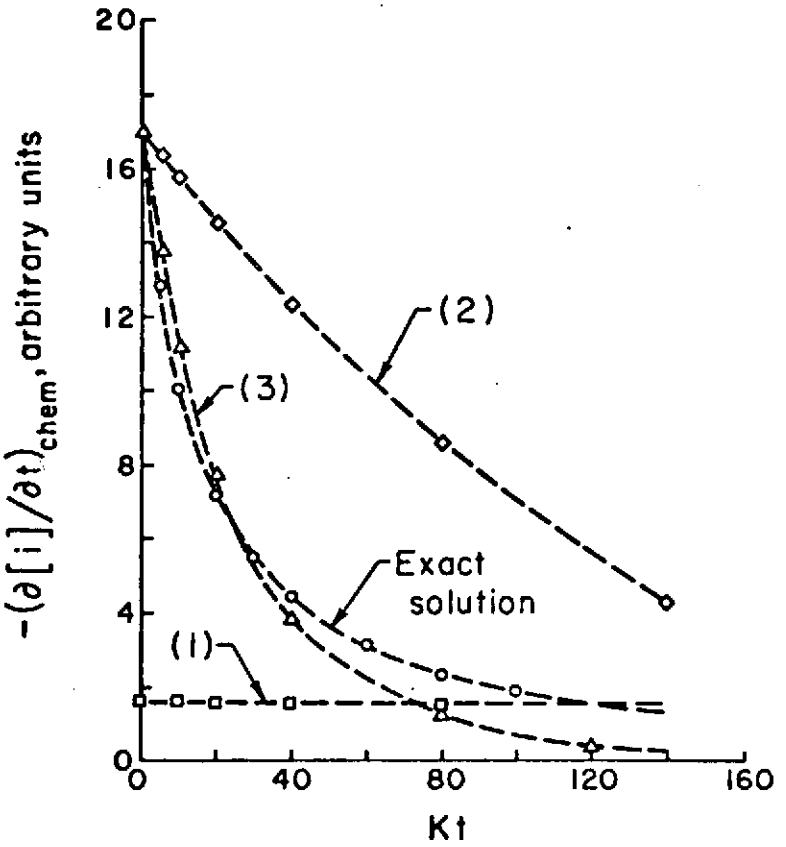

Figure 2. Comparison of predicted vs actual chemical reaction rates under the following conditions:

1) Neglect of concentration fluctuations (uniformly mixed).
2) Neglect of third-order correlations.
3) Inclusion of approximate estimates of third-order correlations.

become less than 1, the fluctuation terms in the chemical kinetics equations become much less than the mean value terms and we recover the classical mean-value chemical kinetics model as a limiting condition on this more general model (ref. 2).

The importance, or lack of importance of these fluctuation terms will be apparent after the chemical submodel is coupled with the second-order turbulent diffusion model. We may note here, however, that the primary effect of inhomogeneous mixing is propagated through the "mixedness" term, $\overline{x'y'}$. This correlation arises primarily through the "folding" of one reactant into the other, without the local, intimate mixing necessary for them to react chemically. When intimate mixing has been achieved, this effect disappears; it has been one of our purposes to assess both the magnitude and duration of $\overline{x'y'}$ in a realistic turbulence and plume configuration situation.

THE MODEL DEVELOPMENT

The Essential Chemistry of the Highly Perturbed Hydrogen-Oxygen-Nitrogen Stratosphere

Recalling that our primary purposes in the present study are to focus attention on the roles of NO_x and H_2O in the determination of the balance of O_3, and to examine the fate of NO_x during the first few hours after NO_x and H_2O are emitted by a single aircraft, we have chosen the following chemical reactions as the essential chemistry of this highly perturbed region of the lower stratosphere:

(R1) $NO + O_3 \xrightarrow{k_2} NO_2 + O_2$ $\qquad k_2 = 4 \times 10^{-15} \dfrac{cm^3}{molec - sec}$ *

(R2) $NO_2 + O \xrightarrow{k_3} NO + O_2$ $\qquad k_3 = 9.1 \times 10^{-12} \dfrac{cm^3}{molec - sec}$ *

(R3) $NO_2 + h\nu \xrightarrow{j_2} NO + O$ $\qquad j_2 = 0 \text{ to } 6.4 \times 10^{-3} \text{ sec}^{-1}$ **

(R4) $O + O_2 + M \xrightarrow{k_1} O_3 + M$ $\qquad k_1[O_2][M] = 2.3 \times 10^{2} \text{ sec}^{-1}$ *

(R5) $O_3 + h\nu \xrightarrow{j_1} O + O_2$ $\quad j_1 = 0$ to 4×10^{-3} sec^{-1} **

(R5') $O_3 + h\nu \xrightarrow{j_1^*} O(^1D) + O_2$ $\quad j_1^* = 0$ to 4×10^{-4} sec^{-1} **

(R6) $O(^1D) + H_2O \xrightarrow{k_5} 2\,OH$ $\quad k_5 = 3.5 \times 10^{-10}$ $\frac{cm^3}{molec - sec}$ *

(R7) $O(^1D) + M \xrightarrow{k_6} O + M$ $\quad k_6 = 7.5 \times 10^{-11}$ $\frac{cm^3}{molec - sec}$ *

(R8) $OH + NO_2 \xrightarrow{k_4} HNO_3$ $\quad k_4 = 2.5 \times 10^{-12}$ $\frac{cm^3}{molec - sec}$ *

(R9) $OH + O_3 \xrightarrow{k_7} HO_2 + O_2$ $\quad k_7 = 2.7 \times 10^{-14}$ $\frac{cm^3}{molec - sec}$ *

(R10) $HNO_3 + h\nu \xrightarrow{j_3} OH + NO_2$ $\quad j_3 = 0$ to 2.3×10^{-7} sec^{-1} *

(R11) $OH + HNO_3 \xrightarrow{k_8} H_2O + NO_3$ $\quad k_8 = 1.3 \times 10^{-13}$ $\frac{cm^3}{molec - sec}$ *

(R12) $HO_2 + O_3 \xrightarrow{k_9} OH + 2O_2$ $\quad k_9 = 3.2 \times 10^{-15}$ $\frac{cm^3}{molec - sec}$ *

This reaction set for twelve chemical species represents, of course, a rather severe truncation of the complete O_3 chemistry in the stratosphere (ref. 12), and the validity of this approximation has not yet been adequately tested against the more complete reaction/chemical-species simulation models. Until this is done, the results derived from the present chemical submodel must be properly qualified.

---

*Garvin (ref. 13)

**Crutzen (ref. 14)

However, these choices of essential chemistry agree well with choices made by other CIAP modelers, extending Lockheed's chemistry model (ref. 15), and catching the essence of the LLL model (ref. 16) for the plume phase chemistry.

The Chemical Submodel

Assuming then that the above reaction set does capture the essential chemistry in a strongly perturbed hydrogen-oxygen-nitrogen stratosphere, we may write the rate equations for each chemical species as follows:

$$\frac{\partial[O_3]}{\partial t} = k_1[O][O_2][M] - k_2[NO][O_3] - (J_1 + J_1^*)[O_3]$$

$$- k_7[OH][O_3] - k_9[HO_2][O_3] \tag{30}$$

$$\frac{\partial[O]}{\partial t} = J_2[NO_2] + J_1[O_3] + k_6[O(^1D)][M] - k_3[NO_2][O]$$

$$- k_1[O][O_2][M] \tag{31}$$

$$\frac{\partial[NO]}{\partial t} = J_2[NO_2] + k_3[NO_2][O] - k_2[O_3][NO] \tag{32}$$

$$\frac{\partial[NO_2]}{\partial t} = J_3[HNO_3] + k_2[NO][O_3] - J_2[NO_2] - k_3[NO_2][O]$$

$$- k_4[NO_2][OH] \tag{33}$$

$$\frac{\partial[HNO_3]}{\partial t} = k_4[NO_2][OH] - J_3[HNO_3] - k_8[HNO_3][OH] \tag{34}$$

$$\frac{\partial[OH]}{\partial t} = 2k_5[O(^1D)][H_2O] + j_3[HNO_3] - k_4[NO_2][OH] - k_7[OH][O_3]$$

$$+ k_9[HO_2][O_3] - k_8[HNO_3][OH] \tag{35}$$

$$\frac{\partial[O(^1D)]}{\partial t} = j_1^*[O_3] - k_5[H_2O][O(^1D)] - k_6[O(^1D)][M] \tag{36}$$

$$\frac{\partial[H_2O]}{\partial t} = k_8[HNO_3][OH] - k_5[O(^1D)][H_2O) \tag{37}$$

$$\frac{\partial[NO_3]}{\partial t} = k_8[OH][HNO_3] \tag{38}$$

$$\frac{\partial[O_2]}{\partial t} = k_2[NO][O_3] + k_3[NO_2][O] + k_7[OH][O_3] + 2k_9[HO_2][O_3]$$

$$+ (j_1 + j_1^*)[O_3] - k_1[O][O_2][M] \tag{39}$$

$$\frac{\partial[HO_2]}{\partial t} = k_7[OH][O_3] - k_9[HO_2][O_3] \tag{40}$$

$$\frac{\partial[M]}{\partial t} = 0 \tag{41}$$

This set of twelve simultaneous partial differential equations represents the nonlinear, closed set which can be derived from reactions (R1) through (R12). This full set can be solved by numerical techniques, given appropriate input values for the twelve chemical species concentrations and the values of the reaction rate constants. Some of the latter are time and position dependent, particularly the photodissociation "constants," but we choose to suppress this variability for our initial calculations. This choice

limits our time integration period to, at most, a few hours, and either sunlit or dark skies.

Before proceeding to these calculations, however, we may take advantage of several approximations which are appropriate to the SST near wake and which greatly simplify both the chemical calculations and the later coupling with source, diffusion, and sink terms. Since some of these approximations constrain the regions of validity of the chemical submodel, they should be carefully observed.

First, we note that the near wake plume is expected to be rich in water vapor and molecular oxygen. We therefore set Eqs. (37) and (39) equal to zero, and treat $[H_2O]$ and $[O_2]$ as constants in the chemical model.

Turning attention now to reactions (R8), (R9), (R11) and (R12), we note that, so long as $[NO_2] > 0.01\ [O_3]$, the completion for OH favors the production of HNO_3 over the production of HO_2. Later, when a substantial amount of NO_2 has been converted to HNO_3, the preferred reaction for OH is with HNO_3, to form H_2O and NO_3 (reaction (R11)). This reaction effectively removes some of the NO and NO_2 from the system. On this basis, we suppress reaction (R12) as a negligible part of this complex system and delete the term $k_9[HO_2][O_3]$ in Eqs. (30) and (35).

For the next set of approximations, we note that O and O('D) are highly reactive chemical species and can be expected to be in approximate equilibrium at all times. Assuming this is the case, we may set Eqs. (31) and (36) equal to zero and solve for the equilibrium concentrations of O and O('D). This yields

$$[O] = \frac{j_2[NO_2] + j_1[O_3] + k_6[O('D)][M]}{k_1[O_2][M] + k_3[NO_2]} \tag{42}$$

and

$$[O('D)] = \frac{j_1^*[O_3]}{k_5[H_2O] + k_6[M]} \tag{43}$$

But the maximum value of $[H_2O]$ expected in the post-vortex plume is about 10^{15} to 10^{16} molecules/cm^3 and, taking $[M] = 10^{18}$ molecules/cm^3, $k_5[H_2O] \ll k_6[M]^*$. Then

$$[O('D)] \simeq \frac{j_1^*[O_3]}{k_6[M]} \tag{44}$$

*This approximation is valid for $[H_2O] \leq 10^{16}$ molec/cm^3

Substituting Eq. (44) in Eq. (42), and noting that $j_1 \simeq 10\, j_1^*$,

$$[O] = \frac{j_2[NO_2] + j_1[O_3]}{k_1[O_2][M] + k_3[NO_2]} \tag{45}$$

Equation (45) can be simplified further by noting that, for $[NO_2] \leq 10^{13}$ (the range of interest), $k_3[NO_2] < k_1[O_2][M]$, and

$$[O] = \frac{j_2[NO_2] + j_1[O_3]}{k_1[O_2][M]} \tag{46}$$

In arriving at these approximations the primary constraint is

$$.01[O_3] < [NO_2] < 10^{13} \text{ molec/cm}^3$$

a range of values of $[NO_2]$ which must be observed in the calculations.

Using all of the above approximations, Eqs. (30) through (41) may be written:

$$\frac{\partial[O_3]}{\partial t} = j_2[NO_2] - k_2[NO][O_3] - k_7[OH][O_3] \tag{47}$$

$$\frac{\partial[NO]}{\partial t} = j_2[NO_2] + k_3[NO_2]\left[\frac{j_2[NO_2] + j_1[O_3]}{k_1[O_2][M]}\right] - k_2[O_3][NO] \tag{48}$$

$$\frac{\partial[NO_2]}{\partial t} = j_3[HNO_3] + k_2[NO][O_3] - j_2[NO_2] - k_3[NO_2]\left[\frac{j_2[NO_2] + j_1[O_3]}{k_1[O_2][M]}\right] - k_4[NO_2][OH] \tag{49}$$

$$\frac{\partial[HNO_3]}{\partial t} = k_4[NO_2][OH] - j_3[HNO_3] - k_8[HNO_3][OH] \tag{50}$$

$$\frac{\partial[OH]}{\partial t} = \frac{2k_5 j_1^*}{k_6[M]}[O_3][H_2O] + j_3[HNO_3] - k_4[NO_2][OH]$$

$$- k_7[O_3][OH] - k_8[HNO_3][OH] \tag{51}$$

Equations (47) through (51) have been solved for the variety of initial conditions which might be expected in the post-vortex SST plume for a period of one to three hours. These calculations (which are appropriate to nonturbulent conditions in the stratosphere) are discussed in the next section. We now complete the model construction by coupling the chemistry submodel with the diffusion model.

The Coupled One-Dimensional Diffusion/Chemistry Model

We adopt a frame of reference which moves with a volume of the plume segment and note that mass continuity for the jth chemical species requires that

$$\frac{d[j]}{dt} = \nu_o \frac{\partial^2[i]}{\partial x_i^2} + \frac{\partial}{\partial x_i} \overline{u_i'[j]'} + \left(\frac{\partial}{\partial t}[j]\right)_{chem} + S_j \tag{52}$$

where the x_i denote orthogonal directions, u_i' are the components of turbulent motion along these directions, and S_j is any local source or sink for j, other than chemical alteration. We take $S_j \equiv 0$ for our present problem, and confine attention to turbulent diffusion in the lateral (y) direction only. Then,

$$\frac{d[j]}{dt} = - \frac{\partial}{\partial y} \overline{v'[j]'} + \left(\frac{\partial}{\partial t}[j]\right)_{chem} \tag{53}$$

and our problem reduces to finding appropriate models for each term on the right-hand side of Eq. (53) and for each of the five chemical species retained as variables in the chemical submodel. These modeling techniques are provided by previous development of second-order closure techniques for turbulent diffusion processes (ref. 1) and inhomogeneous chemistry (ref. 2).

However, in order to keep the number of simultaneous equations manageable, we invoke two more approximations in the chemistry model. First we assume that OH is always in equilibrium, and second, we neglect the second-order correlations of concentration fluctuations in the chemistry, i.e., we use mean value chemistry only. The importance of this latter assumption can be rigorously tested only when it is deemed desirable to program the more complete model for a large, high speed computer. However, calculations on simpler reaction systems (H_2O is neglected) in which the second-order correlation, or "mixedness" term is retained have shown this term alters the reaction rate predicted by mean value chemistry by no more than about thirty per cent for typical SST plumes and, in turbulent flow, persists for only a matter of a few tens of minutes (see Appendix A). Given the degree of uncertainty in other parts of the system, e.g.g., reaction rate constants, initial species concentrations, turbulence intensity, etc., we are justified in neglecting this effect in these preliminary calculations for the full H-N-O system.

The justification for assuming that OH is always in chemical equilibrium must be based on its high degree of reactivity and therefore its small characteristic chemical time in comparison with O_3, NO, NO_2, and HNO_3. Since this assumption is not made in the full chemical submodel, we are in a position to assess its validity by comparing calculations made with that model with those made with the coupled model when the turbulent diffusion is taken as zero. Adopting this assumption, we have from Eq. (22),

$$[OH] = \frac{\frac{2k_5 j_1^*}{k_6[M]}[O_3][H_2O] + j_3[HNO_3]}{k_4[NO_2] + k_7[O_3] + k_8[HNO_3]} \qquad (54)$$

A comparison of k_4, k_7, and k_8 shows that, so long as $[NO_2] > .01[O_3]$ or $[HNO_3] > 0.1[O_3]$, we may safely neglect the term $k_7[O_3]$ in Eq. (54), although we retain it in Eq. (47). Finally, we note that in the early plume phase, where [OH] can be expected to be relatively large, the primary mechanism for the destruction of HNO_3 is by reaction with OH, not by photodissociation. We therefore neglect $j_3[HNO_3]$ in favor of $k_8[HNO_3][OH]$ wherever they appear.

Under these conditions, the coupled chemistry/diffusion model becomes:

$$\frac{d[O_3]}{dt} = - \frac{\partial}{\partial y} \overline{v'[O_3]'} + j_2[NO_2] - k_2[NO][O_3]$$

$$- k_7[O_3] \left[\frac{2k_5 \, j_1^*[O_3][H_2O]}{k_6[M](k_4[NO_2] + k_8[HNO_3])} \right] \quad (55)$$

$$\frac{d[NO]}{dt} = - \frac{\partial}{\partial y} \overline{v'[NO]'} + j_2[NO_2]$$

$$+ \frac{k_3[NO_2]}{k_1[O_2][M]} \left[j_2[NO_2] + j_1[O_3] \right] - k_2[O_3][NO] \quad (56)$$

$$\frac{d[HNO_3]}{dt} = - \frac{\partial}{\partial y} \overline{v'[HNO_3]'} + \frac{k_4[NO_2] - k_8[HNO_3]}{k_4[NO_2] + k_8[HNO_3]} \times$$

$$\left[\frac{2k_5 \, j_1^*[O_3][H_2O]}{k_6[M]} \right] \quad (57)$$

$$\frac{d[NO_x]}{dt} = - \frac{\partial}{\partial y} \overline{v'[NO_x]'} - k_8[HNO_3] \left[\frac{2k_5 \, j^*[O_3][H_2O]}{k_4[NO_2] + k_8[HNO_3]} \right] \quad (58)$$

$$\frac{d[H_2O]}{dt} = - \frac{\partial}{\partial y} \overline{v'[H_2O]'} \quad (59)$$

$$[NO_2] = [NO_x] - [NO] - [HNO_3] \quad (60)$$

and it is understood that all unprimed chemical species concentrations are ensemble averages.

Having chosen to suppress the higher-order moments in the chemistry submodel, we may write down the diffusion equations directly from Donaldson (ref. 1) in the form

$$\frac{\partial \overline{v'[j]'}}{\partial t} = \overline{v'^2}\,\frac{\partial [j]}{\partial y} + \frac{g}{T_o}\,\overline{T'[j]'} + v_2\,\frac{\partial}{\partial y}\left(\Lambda_2 q\,\frac{\partial \overline{v'[j]'}}{\partial y}\right) - \frac{q}{\Lambda_1}\,\overline{v'[j]'} \tag{61}$$

$$\frac{\partial \overline{T'[j]'}}{\partial t} = \overline{v'[j]'}\,\frac{\partial \overline{T}}{\partial y} - \overline{v'T'}\,\frac{\partial [j]}{\partial y} + \frac{\partial}{\partial y}\left(\Lambda_2 q\,\frac{\partial \overline{T'[j]'}}{\partial y}\right) \tag{62}$$

$$\frac{\partial \overline{w'T'}}{\partial t} = -\overline{v'^2}\,\frac{\partial \overline{T}}{\partial y} + \frac{g}{T_o}\,\overline{T'^2} + 2\,\frac{\partial}{\partial y}\left(\Lambda_2 q\,\frac{\partial \overline{v'T'}}{\partial y}\right) + \frac{1}{\rho_o}\,\frac{\partial}{\partial y}\left(\rho_o \Lambda_3 q\,\frac{\partial \overline{v'T'}}{\partial y}\right) - \frac{q}{\Lambda_1}\,\overline{v'T'} \tag{63}$$

and

$$\frac{\partial \overline{T'^2}}{\partial t} = -2\overline{v'T'}\,\frac{\partial \overline{T}}{\partial y} + \frac{\partial}{\partial y}\left(\Lambda_2 q\,\frac{\partial \overline{T'^2}}{\partial y}\right) \tag{64}$$

where molecular diffusion has been neglected. Since the chemical species do not appear in Eqs. (63) and (64), these are derived from the turbulence model and used as standard inputs to the five pairs of diffusion equations denoted by Eqs. (61) and (62). The latter are, in turn, coupled with the appropriate chemistry terms to provide a set of fifteen differential equations which are to be solved for the values of $[O_3]$, $[NO]$, $[NO_2]$, $[HNO_3]$, and $[H_2O]$ as a function of position in the plume, y, and time after vortex decay, t. The inputs required for the turbulence part of this model are the turbulent kinetic energy, q^2, the lateral component of q^2, $\overline{v'^2}$, and the scale lengths, Λ_i. The reader interested in the details of this part of the model is referred to ref. 1 and 2. The main point to note here is that the diffusion scale length is keyed to the lateral dimension of the plume, giving a scale-dependent

diffusion process analogous to that developed by Walton (ref. 17).

In the present use of this coupled model we are more interested in exploring the range of possible turbulence and chemistry processes in the near SST wake than in duplicating any single event. The lack of validation data is not a severe handicap in this initial sensitivity analysis; choosing which of the many possible conditions actually does occur, and validating the model's predictions for those cases, does of course depend heavily on data which are not yet available.

PRELIMINARY MODEL CALCULATIONS

Chemistry Only

Since one of the primary problems addressed by CIAP is the chemical reactions among NO_x, H_2O, and O_3, particularly as these effect the balance of O_3 in the stratosphere, we have exercised the chemistry model extensively to determine the rates and time-integrated reactions for these components during their first few hours in the sunlit stratosphere. Recall one of our primary purposes here is to estimate the chemical form of the oxides of nitrogen and how they are transformed during these first few hours. For these preliminary calculations we have programmed Eqs. (47) - (51) for computer solutions and have calculated the time-dependent values of $[O_3]$, $[NO]$, $[NO_2]$, and $[HNO_3]$ for all combinations of the following initial conditions:

$$[O_3]_o = 5 \times 10^{12},\ 10^{12},\ \text{and}\ 10^{11}\ \text{molecules/cm}^3$$

$$[H_2O]_o = 3.5 \times 10^{17},\ 1.7 \times 10^{17},\ 3.5 \times 10^{16},\ 3.5 \times 10^{14},\ \text{and}\ 3.5 \times 10^{13}\ \text{molecules/cm}^3$$

$$[NO_x]_o = [NO]_o + [NO_2]_o = 10^{13},\ 5 \times 10^{12},\ 2 \times 10^{12},\ 10^{12},\ \text{and}\ 10^{11}\ \text{molecules/cm}^3$$

$$[NO]_o/[NO_2]_o = 0,\ 1,\ \text{and}\ 3$$

$$[HNO_3]_o = 0$$

The reaction rate constants were assigned values given with reactions (R1)-(R12), and the photolysis constants, j_1, j_2, and j_1^* were assigned values of 4×10^{-4}, 6.4×10^{-3}, and 4×10^{-5}, respectively. Approximately 200 calculations were performed for a time integration period of 2.5 hours. Typical time histories of chemical species concentrations are shown in Fig. 3; in addition to these primary outputs, the program also provided the time rate of change of species concentration and the characteristic time for these changes, also as a function of time.

As an initial framework for examining this multi-variate system, and for an early appraisal of HNO_3 formation in this photochemical simulation, we have determined the combinations of $[O_3]_o$, $[NO_x]_o$, and $[NO]_o/[NO_2]_o$ for which more than ten per cent of the initial NO_x is converted to HNO_3 in 2.5 hours. These delineations are displayed in Fig. 4. The following qualitative picture of the probability of significant HNO_3 production is immediately evident:

1. The probability of HNO_3 formation increases with increasing $[H_2O]$ and increasing $[O_3]_o$ and decreases with increasing $[NO_x]$.

2. HNO_3 formation is less sensitive to $[NO]_o/[NO_2]_o$ than to $[O_3]_o$, but the sensitivity to the former increases as $[NO_x]$ and $[H_2O]$ increase and $[O_3]$ decreases.

3. For $[NO_x] \geq \sim 5 \times 10^{12}$ molecules/cm^3 the probability of HNO_3 formation becomes vanishingly small.

The combinations of $[O_3]_o$, $[NO_x]$, and $[NO]_o/[NO_2]_o$ used in constructing Fig. 4 bracket essentially all conceivable values which could be encountered in the SST exhaust plume. However, as a preliminary test of the sensitivity of HNO_3 formation to the photolysis rates, approximately 100 additional calculations were made for the same initial conditions, but j_1^* was increased to 1.6×10^{-4} sec^{-1} and j_2 was decreased to 6.4×10^{-4} sec^{-1}. The combinations of $[O_3]_o$, $[NO_x]$, $[H_2O]$, and $[NO]_o/[NO_2]_o$ which led to the conversion of at least ten per cent of the NO_x to HNO_3 in 2.5 hours are shown in Fig. 5. The same general results described above are still evident, but the probability of significant HNO_3 formation is now considerably enhanced for lower values of $[O_3]_o$ and moderate to large values of H_2O. This result, of course, reflects the greater abundance of $O(^1D)$ and consequent formation of OH, and then HNO_3.

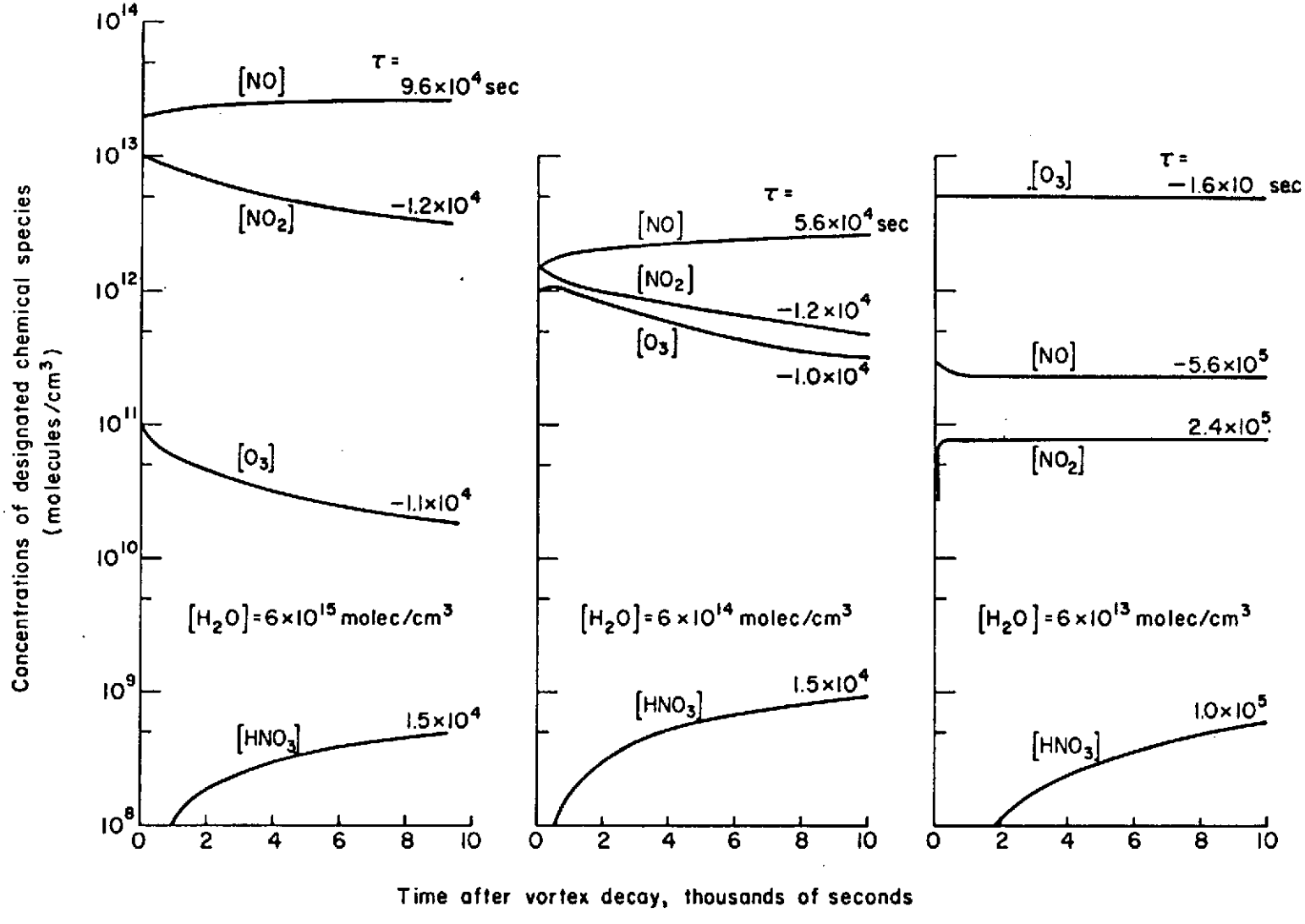

Figure 3. A typical time history of the concentrations of O_3, NO, NO_2 and HNO_3.

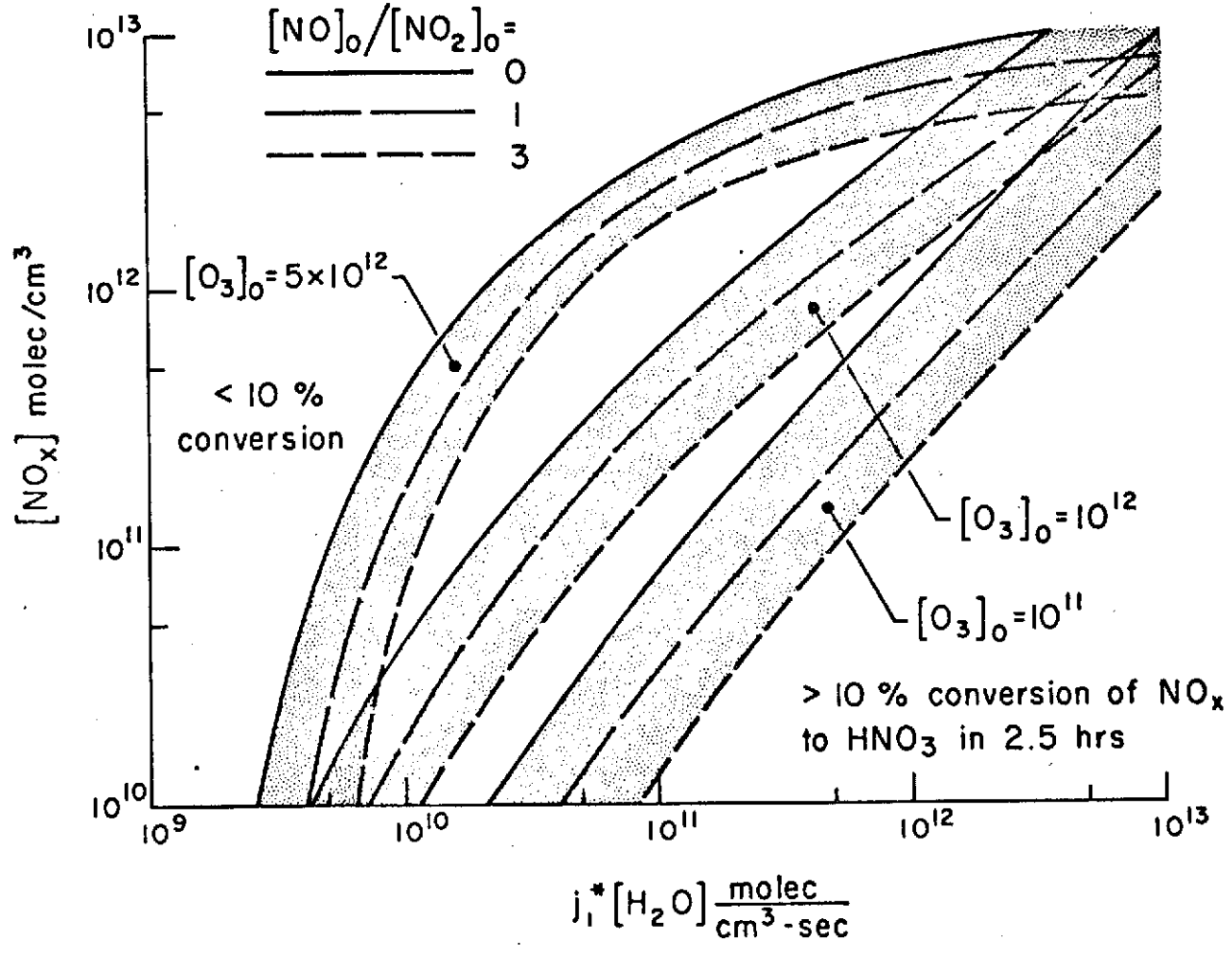

Figure 4. The threshold values of initial $[O_3]$, $j_1^*[H_2O]$, and $[NO]/[NO_2]$ which produce more than 10 per cent conversion of NO_x to HNO_3 in 2.5 hrs. ($j_1^* = 4\times10^{-5}$ sec^{-1} and $j_2 = 6.4\times10^{-4}$ sec^{-1}).

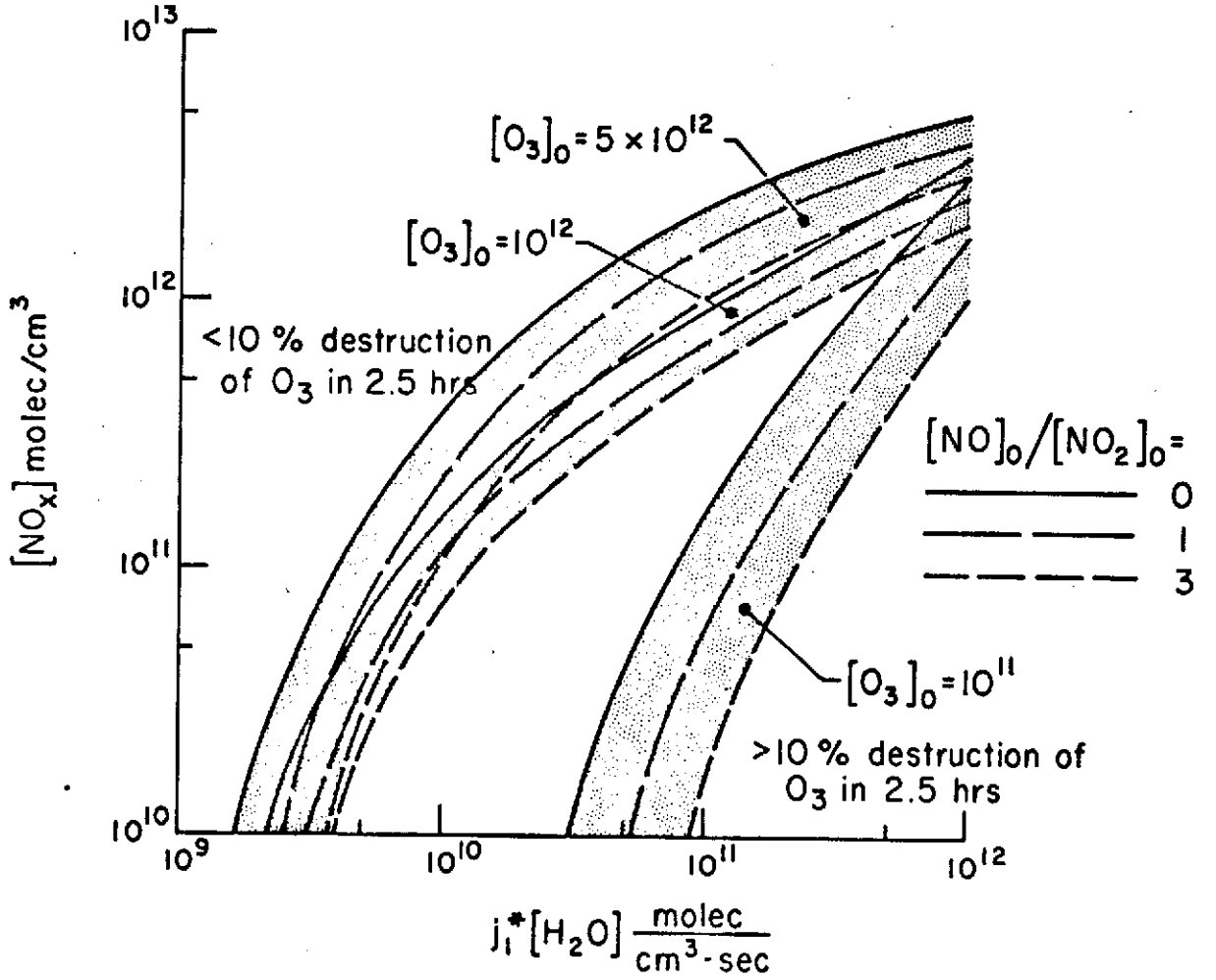

Figure 5. The threshold values of initial $[O_3]$, $j_1^*[H_2O]$, and $[NO]/[NO_2]$ which produce more than 10 per cent conversion of NO_x to HNO_3 in 2.5 hrs. ($j_1^* = 4 \times 10^{-4}$ sec^{-1} and $j_2 = 6.4 \times 10^{-4}$ sec^{-1}).

Even with the elevated value of j_1^*, the controlling upper limit of $[NO_x]$ is still very evident. An inspection of the calculations quickly reveals that the reason for this limit is to be found in the abrupt depletion of O_3 in the photochemical system when $[NO_x]$ exceeds about 10^{12} molecules/cm^3. In order to show this, we have analyzed the first set of calculations (daily average photolysis constants) for the combinations of $[NO_x]$, $[H_2O]$, and $[NO]_o/[NO_2]_o$ for which $[O_3]$ is depleted to less than one-half its initial value in 2.5 hours. These delineations are shown in Fig. 6, and they show the abrupt demise of O_3 for values of $[NO_x] > \sim 5 \times 10^{12}$ molecules/cm^3 and $j_1^*[H_2O] < 10^{12}$ molecules/cm^3 sec. An interesting interplay of H_2O and NO_x sets in when $j_1^*[H_2O] > 10^{12}$ molecules/cm^3 sec. First, the threshold of $[NO_x]$ for O_3 destruction greater than 50 per cent is raised, and then, for $j_1^*[H_2O] > \sim 5 \times 10^{12}$ molecules/cm^3 sec, this measure of the destruction of O_3 becomes essentially independent of $[NO_x]$. Evidently, the first role of H_2O in the O_3 balance is to inhibit the destruction of O_3 by NO_x, by the simple expedient of converting NO_x to HNO_3, and then at large values of $[H_2O]$, H_2O alone is capable of annihilating O_3 through the OH chain.

The primary preliminary result to be noted at this stage, however, is that significant formation of HNO_3 can occur with values of $[O_3]$, $[H_2O]$, and $[NO_x]$ which could occur and persist for 2.5 hours in the initial SST exhaust plume. However, given the sensitivity of HNO_3 formation to the existence of O_3 in the plume and the upper bounds on $[NO_x]$ and $[H_2O]$ we must inquire more closely regarding both the initial concentrations and the effect of turbulent mixing before any definitive application of these results can be made to the problem of the SST plume.

Before proceeding to this larger problem, a more quantitative analysis of the conversion of NO_x to HNO_3 and the destruction of O_3, due to chemical reactions only, is possible and instructive. Turning to the destruction rate for O_3 first, we consider the characteristic time for O_3 destruction, τ_{O_3}, as defined by

$$\tau_{O_3} = -\left(\frac{1}{[O_3]}\frac{d[O_3]}{dt}\right)^{-1} \qquad (65)$$

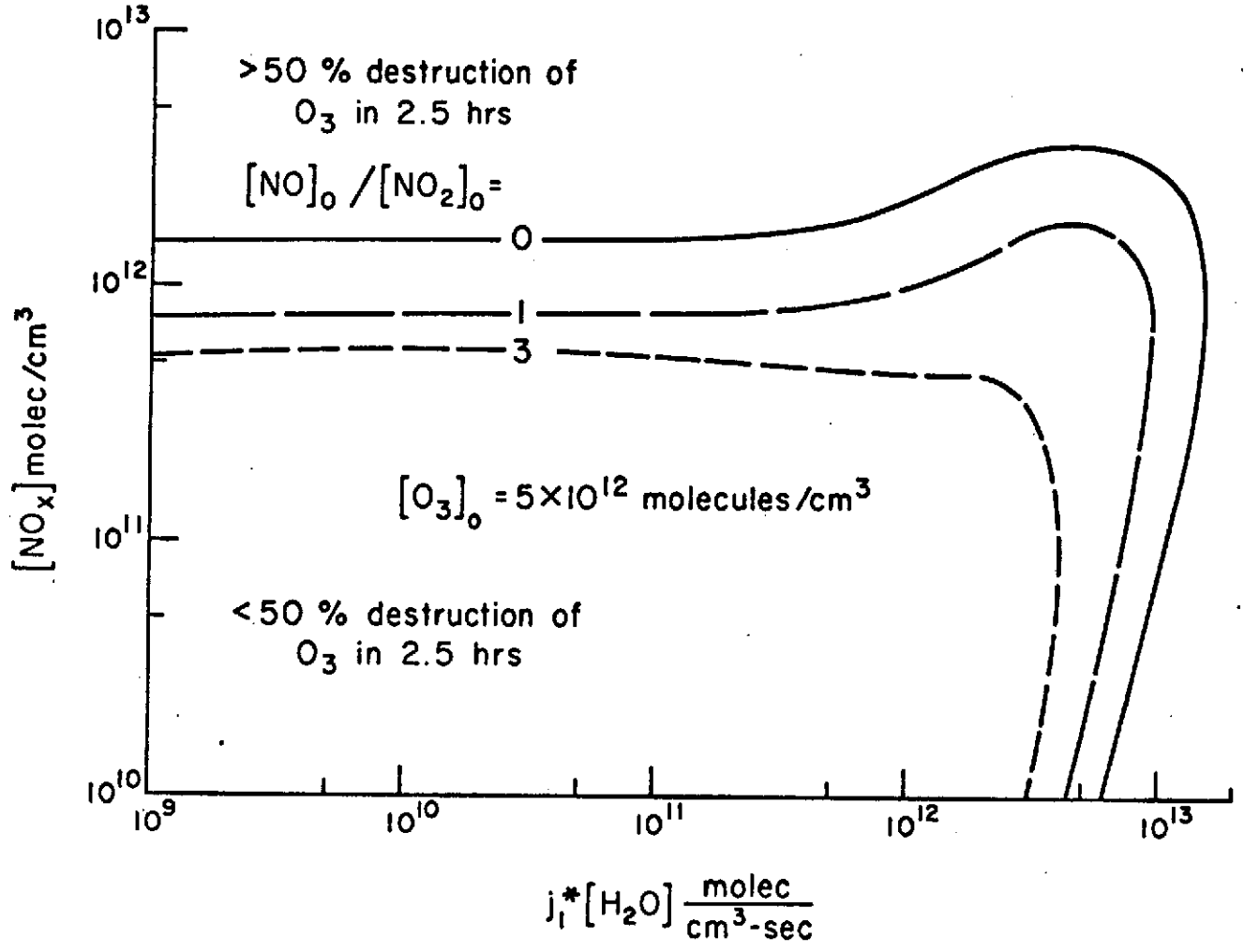

Figure 6. The threshold initial values of $[NO_x]$, $j_1^*[H_2O]$, and $[NO]/[NO_2]$ which produce more than a 50 per cent depletion in $[O_3]$ in 2.5 hrs. ($j_1^* = 4 \times 10^{-5}$ sec^{-1} and $j_2 = 6.4 \times 10^{13}$ sec^{-1}).

and as calculated by the chemical model at t = 2.5 hours. The behavior of τ_{O_3} as a function of $[O_3]_o$, $[NO_x]$, and $j_1*[H_2O]$ is shown in Figs. 7, 8, and 9. The interplay of H_2O and NO_x in controlling the rate of destruction of O_3 is now very clear. Three distinct regimes, as delineated by the solid lines in Figs. 7, 8, and 9 are recognized. First for $[NO_x]/[O_3]_o \leq j_1*[H_2O]/5 \times 10^{12}$, τ_{O_3} is independent of $[NO_x]$ and is inversely proportional to $j_1*[H_2O]$. In the second regime, τ_{O_3} increases with increasing $[NO_x]$ until the critical value for NO_x destruction of O_3 is approached. This critical limit of NO_x depends upon both $[O_3]_o$ and $j_1*[H_2O]$ in a somehwat more complicated way than was true for the delineation of the boundary between regimes one and two.

We should also note in passing, although not included in the calculations, that at normal background values of $[O_3] = 5 \times 10^{12}$, $[NO_x] \simeq 10^{10}$, and $j_1*[H_2O] \simeq 10^8$, the NO_x limit on O_3 destruction clearly predominates over any H_2O effect. Again of peripheral interest to the intent of the present study, these simulations point out that the characteristic time for O_3 destruction in near-background concentrations of NO_x and O_3 is at least of the order of thousands to tens of thousands of hours. If these estimates have any validity, they point to the importance of the residence time of SST generated NO_x in the stratosphere as the single most important parameter in estimating the long-term effects of these emissions on stratospheric O_3 content.

Finally, these preliminary and exploratory calculations provide a more quantitative analysis of the conversion of NO_x to HNO_3. Again, we choose to examine this process at 2.5 hours after vortex decay and for the conditions of daily average photolysis, with other conditions chosen to bracket all reasonable combinations of $[H_2O]$ and $[NO_x]$ in the initial, post-vortex SST plume. The fraction of NO_x converted to HNO_3 during a period of 2.5 hours for values of $[H_2O]$ and $[NO_x]$ ranging from approximately ten times background to one thousand times background, are shown in Figs. 10, 11, and 12. A casual inspection of these results points up quickly that combinations of large values of $[O_3]_o$ and $[H_2O]$, matched with relatively low values of $[NO_x]$, produce very large conversions of NO_x to HNO_3 in 2.5 hours. The larger question is, of course, whether or not these combinations can be produced and sustained in the early SST plume. In order to further emphasize this very important role of the joint values of $[O_3]_o$, $[NO_x]$ and

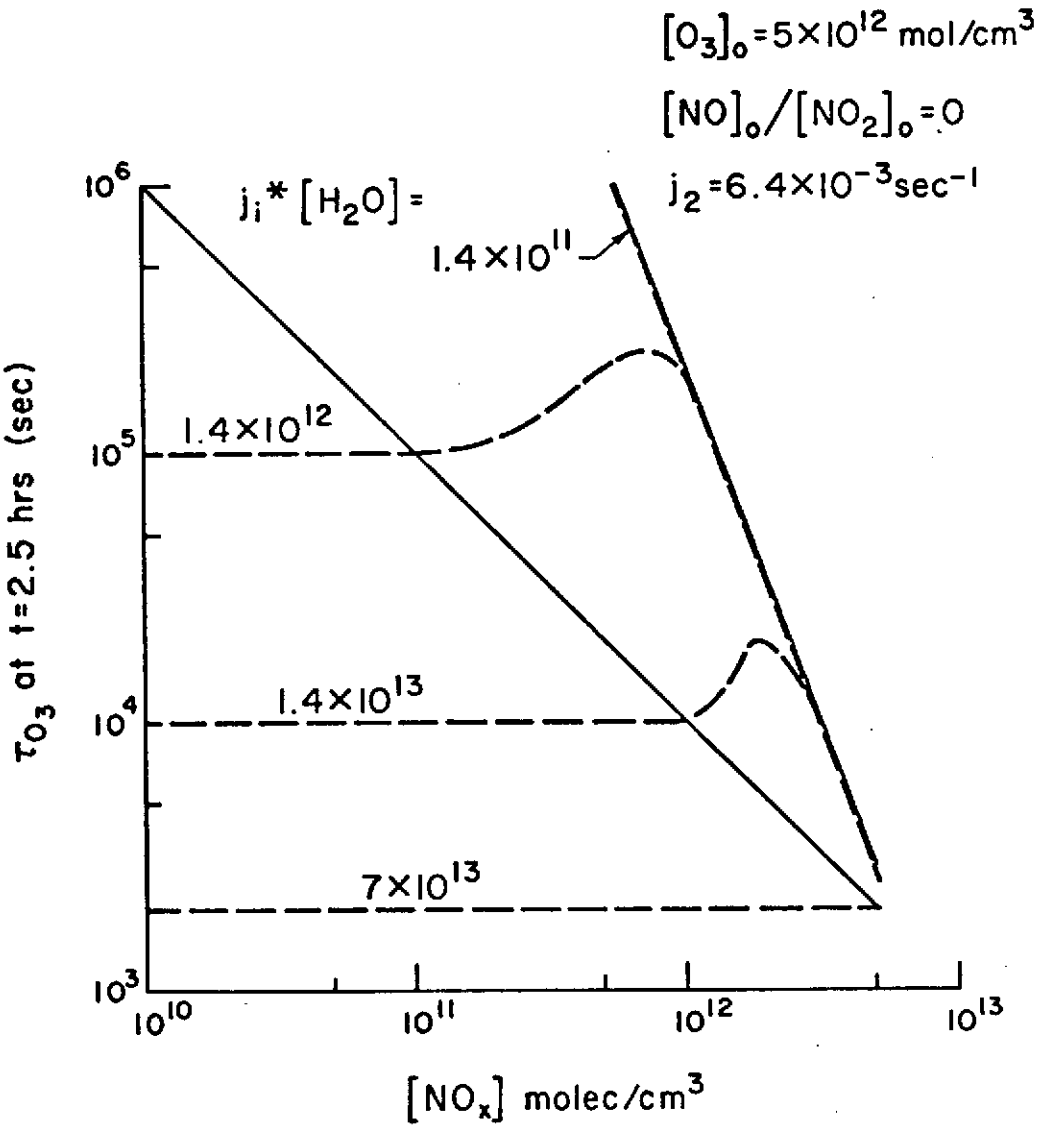

Figure 7. The characteristic time for the depletion of $[O_3]$, at 2.5 hrs, as a function of the initial values of $[NO_x]$, $j_1*[H_2O]$, and for $[O_3]_o$ = 5×10^{12} molecules/cm^3.

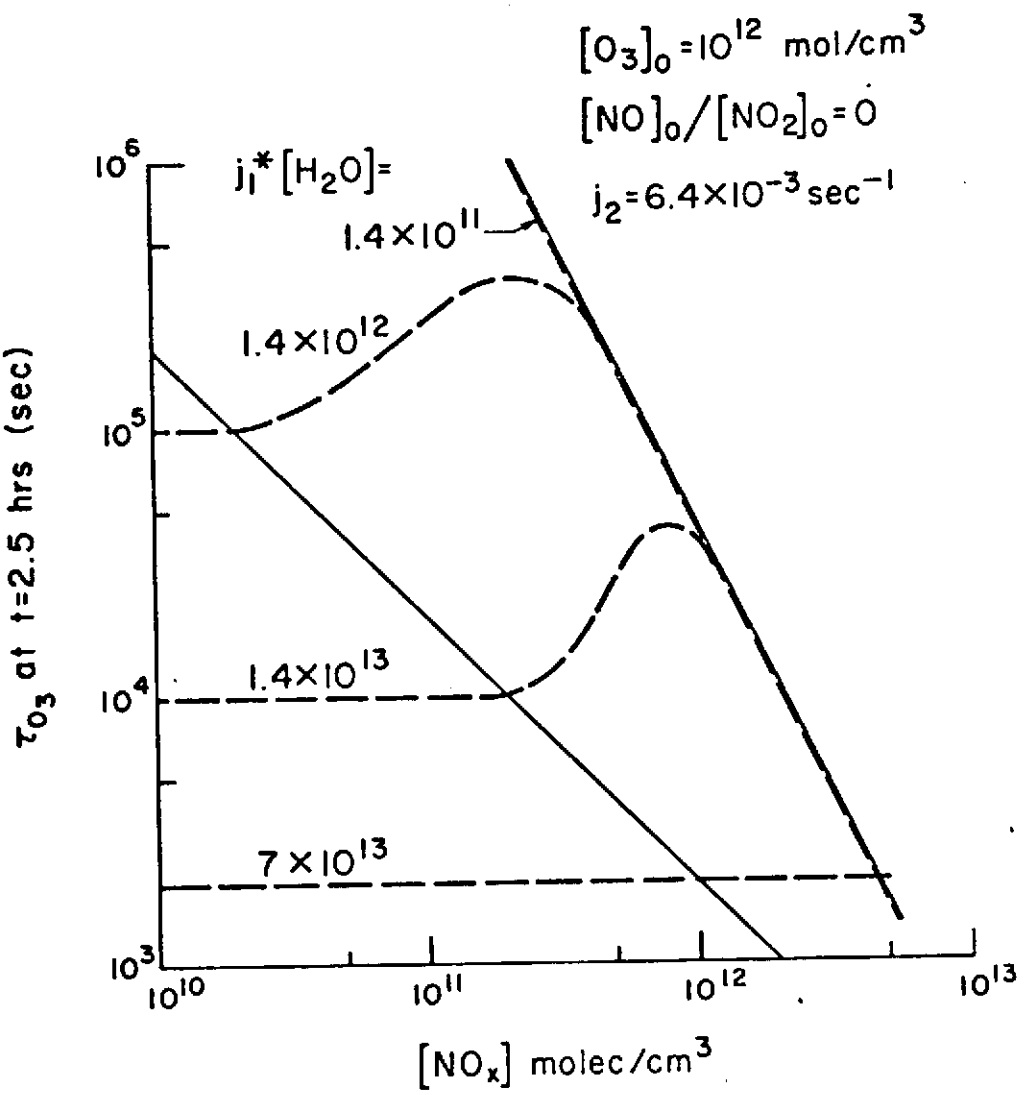

Figure 8. The characteristic time for the depletion of $[O_3]$, at 2.5 hrs, as a function of the initial values of $[NO_x]$, $j_1*[H_2O]$, and for $[O_3]_o = 10^{12}$ molecules/cm^3.

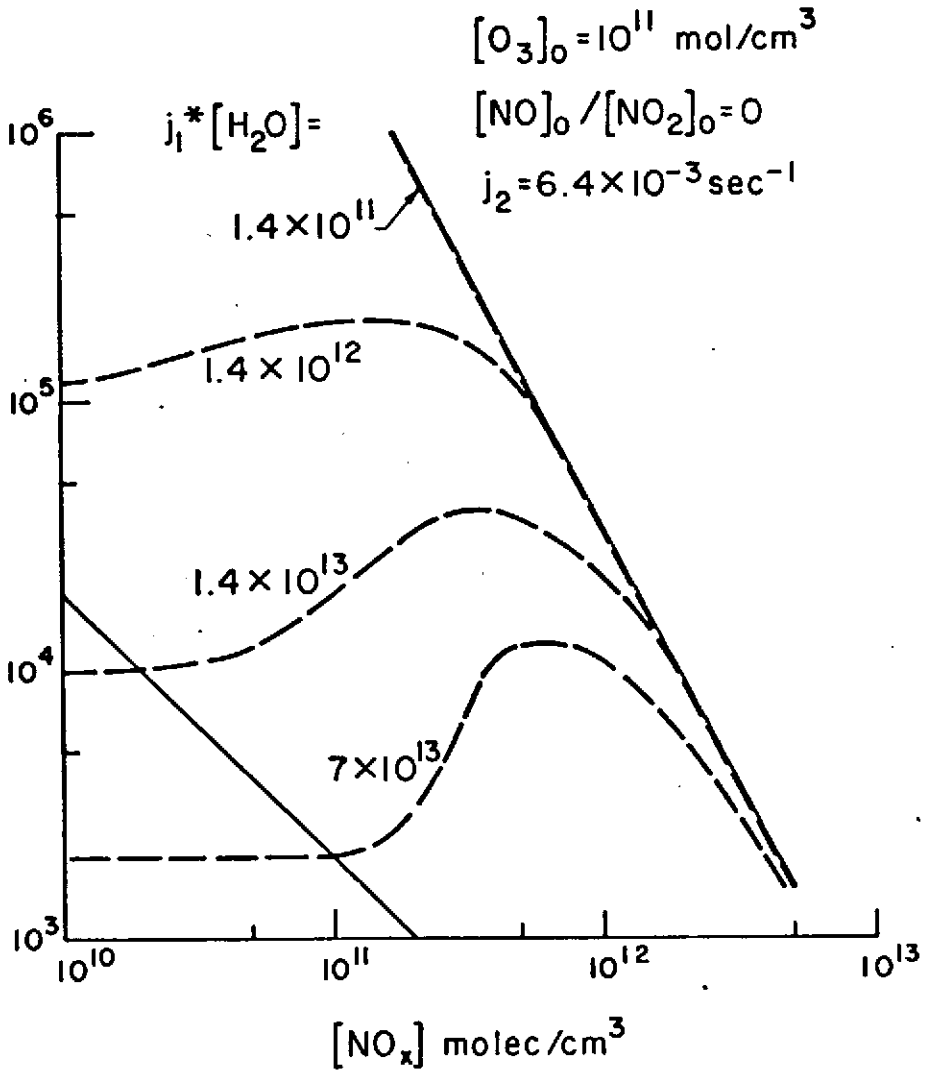

Figure 9. The characteristic time for the depletion of $[O_3]$, at 2.5 hrs, as a function of the initial values of $[NO_x]$, $j_1 * [H_2O]$, and for $[O_3]_o = 10^{11}$ molecules/cm^3.

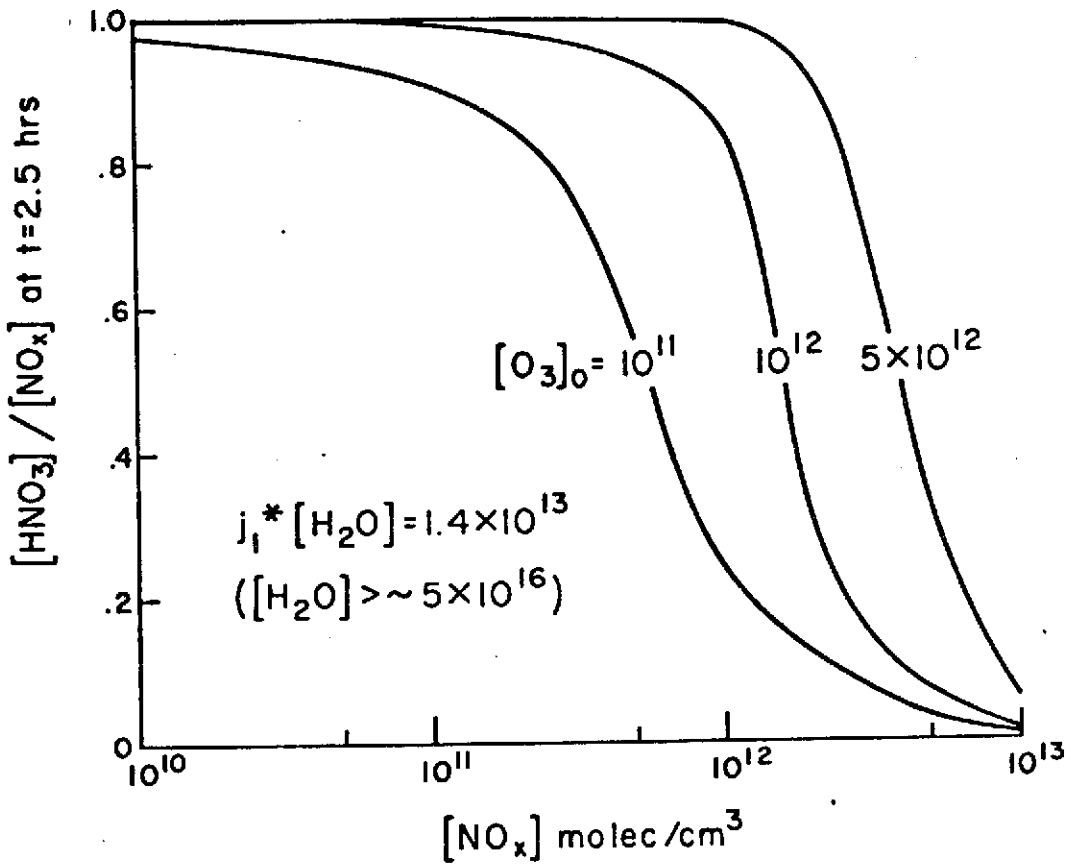

Figure 10. The fraction of NO_x converted to HNO_3 in 2.5 hrs as a function of the initial $[NO_x]$, $[O_3]$, and $j_1^*[H_2O] = 1.4 \times 10^{13}$ molecules/cm^3 sec.

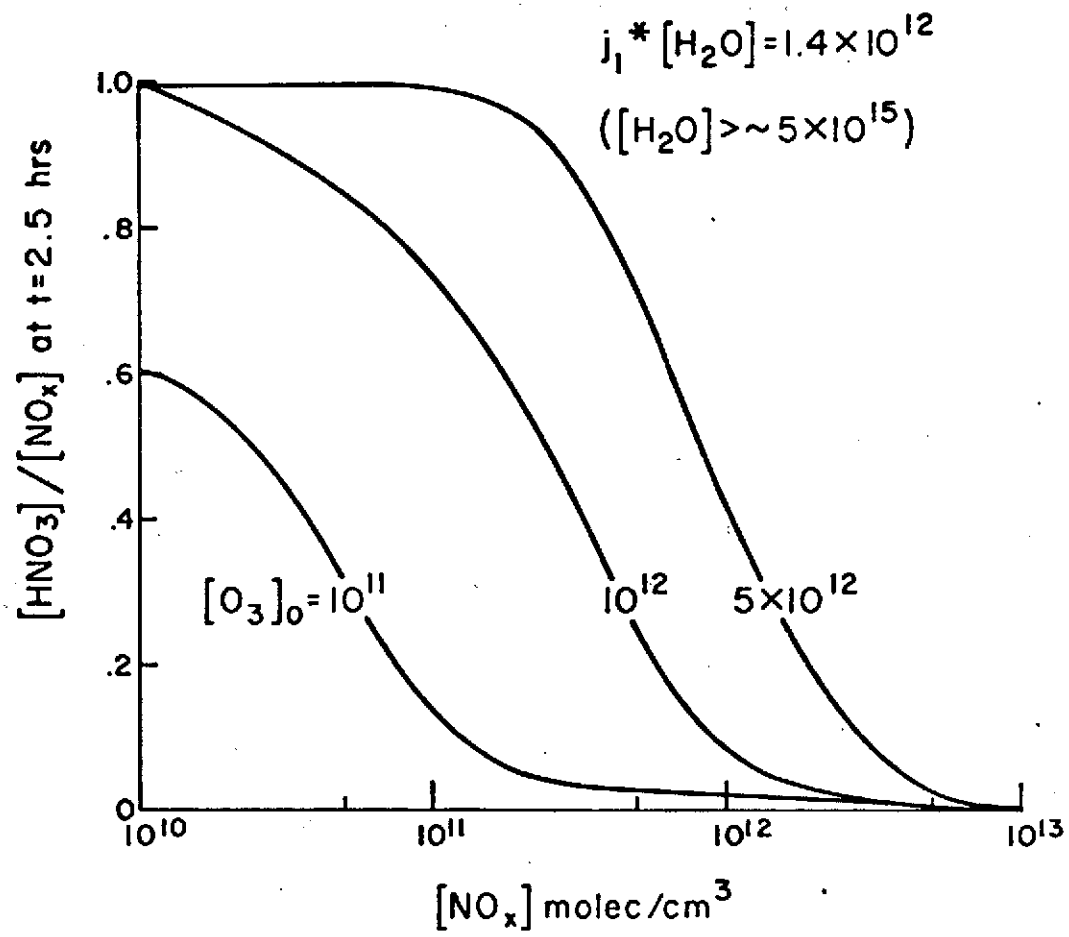

Figure 11. The fraction of NO_x converted to HNO_3 in 2.5 hrs as a function of the initial $[NO_x]$, $[O_3]$, and $j_1^*[H_2O] = 1.4 \times 10^{12}$ molecules/cm^3 sec.

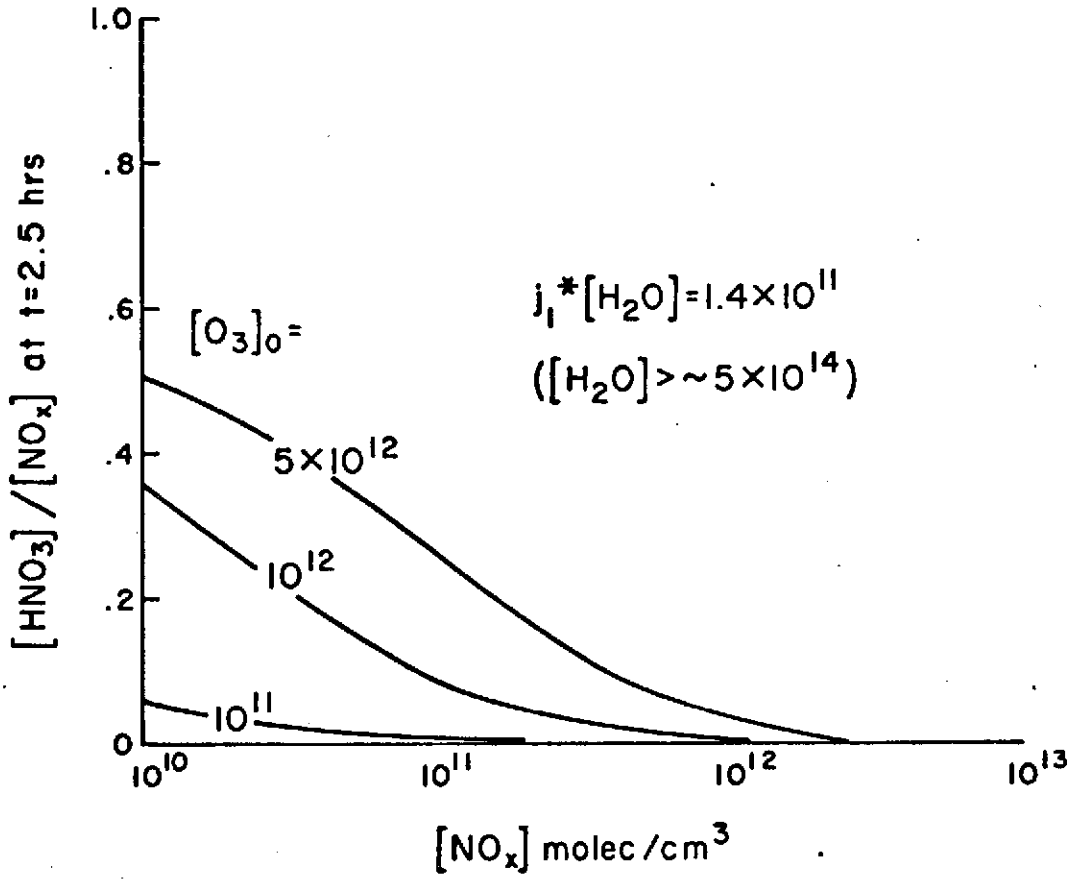

Figure 12. The fraction of NO_x converted to HNO_3 in 2.5 hrs as a function of the initial $[NO_x]$, $[O_3]$, and $j_1^*[H_2O] = 1.4 \times 10^{11}$ molecules/cm^3 sec.

$[H_2O]$ in the production of HNO_3, from chemistry alone, these calculations have been summarized in still another format in Fig. 13. Here the combinations of $[O_3]_o$, $[NO_x]$, and $[H_2O]$ which can chemically produce the conversion of NO_x to HNO_3 greater than given fractions of $[NO_x]$ are displayed. These results are, in turn summarized in Fig. 14 to show the combinations of $[O_3]_o$ and $[NO_x]$ which, in association with two values of $[H_2O]$, can convert more than 10 and 50 per cent of the initial NO_x to HNO_3 in 2.5 hrs. These results, although interesting in their own right, are sobering when considered in the context of the initial SST plume conditions. They say, in effect, that from self-regenerative chemistry alone (no mixing or dilution), a large fraction of the NO_x is quickly converted to HNO_3 only if $[NO_x]$ and $[H_2O]$ two to three orders of magnitude above background characterize the post-vortex plume and, of course, are maintained for 2 to 3 hours.

It seems clear enough that reliable estimates of the vortex decay period dilution of the initial SST plume, in order to establish the initial conditions on $[O_3]$, $[NO_x]$, $[NO]/[NO_2]$, and $[H_2O]$, now become critical to the present study. In addition, estimates of the dilution or redistribution of these quantities during the first few hours after vortex decay are also critical, and must be coupled with the chemical system simulation if reliable estimates of <u>total</u> NO_x conversion to HNO_3 within the plume are to be had.

The Problem of Vortex Decay and the Initial Conditions for the Post-Vortex SST Exhaust Plume

Although second-order closure modeling of the behavior and decay of aircraft-induced vortices and submarine wakes in oceanic thermoclines shows promise of quantitative predictions in the future, it is generally agreed that detailed predictions of the turbulence fields associated with vortex-pair breakup and decay are presently beyond the state of the art. In order to lend some degree of realism to the sensitivity analyses which follow, we have attempted to estimate the entrainment of O_3 and the conversion of NO to NO_2 during the vortex decay period, using the coupled chemistry and diffusion model, and approximating the decaying turbulence field by a short-lived, but <u>constant</u> value of the turbulent kinetic energy. In addition, we have assumed that the dimensions of the turbulence field induced by vortex decay are large compared with the width of the exhaust plume which is embedded in this turbulence field. These assumptions are, at best, only gross approximations of the real situation.

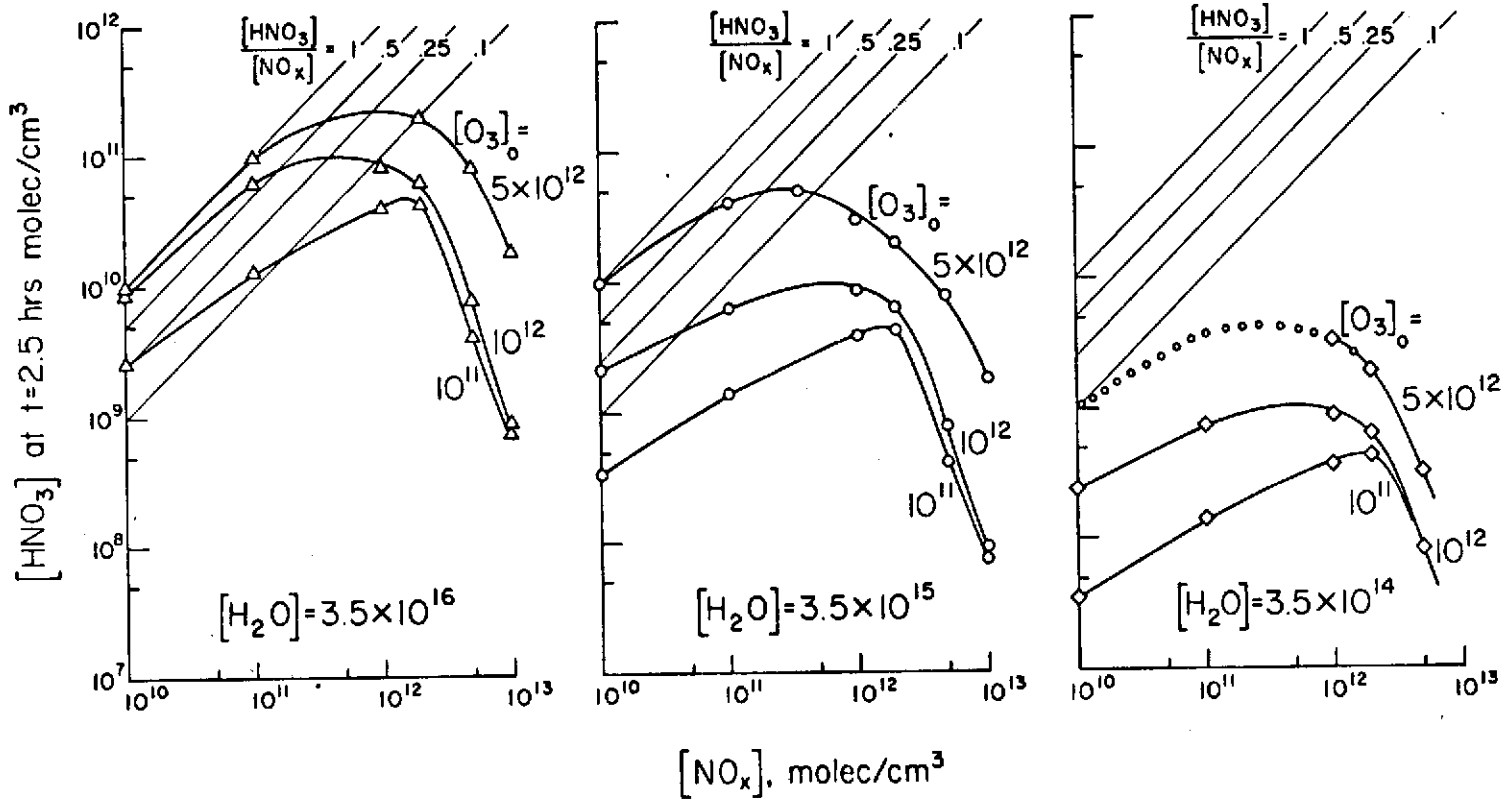

Figure 13. HNO_3 formation at t = 2.5 hrs as a function of initial conditions. Note particularly the fraction of NO_x converted to HNO_3 and the controlling nature of $[NO_x]$ on the conversion process.

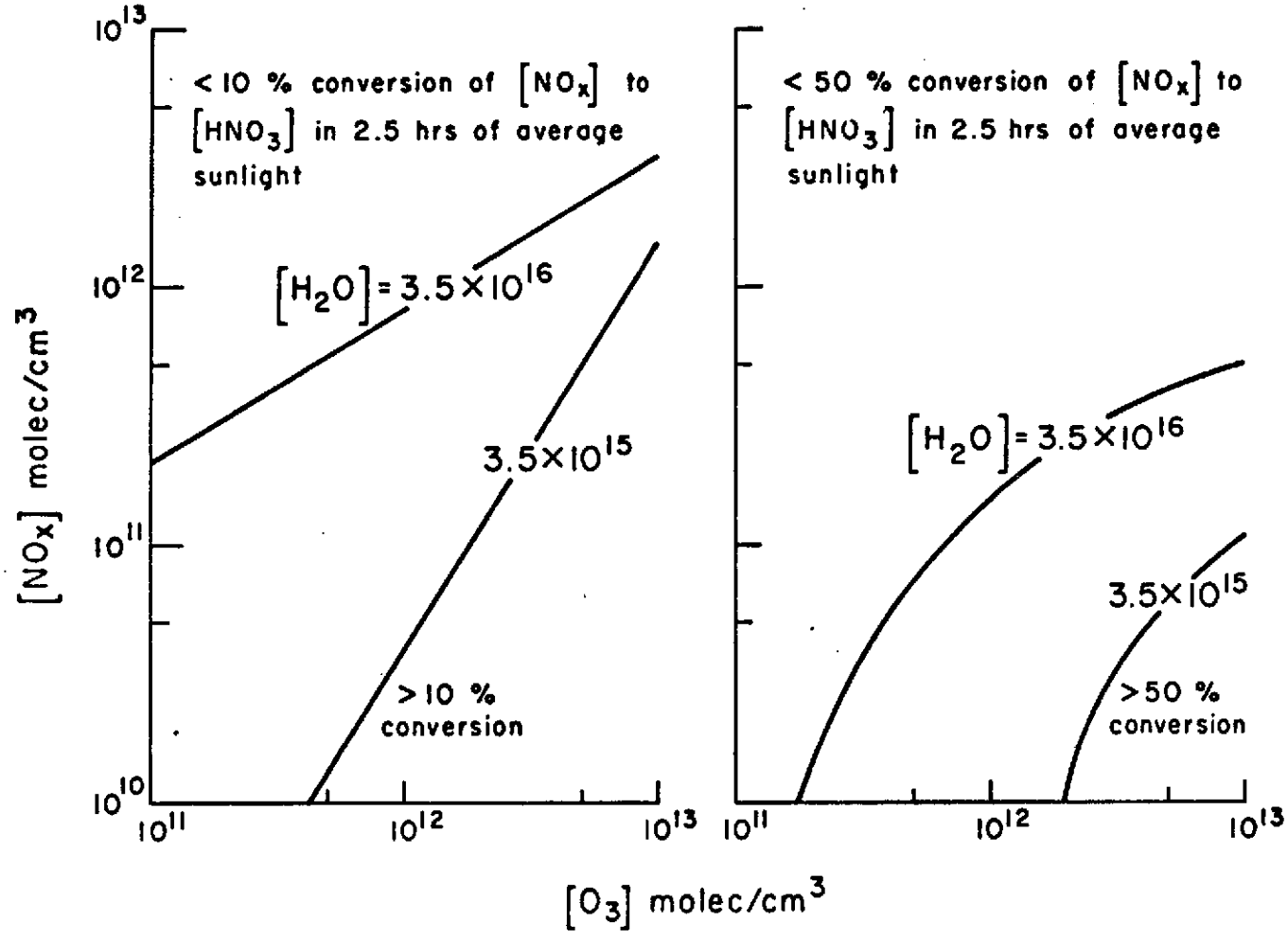

Figure 14. Threshold limits of the initial values of $[O_3]$ and $[NO_x]$ on the conversion of NO_x to HNO_3 in average sunlight and in a period of 2.5 hrs.

However, they do permit an estimate of whether or not turbulent mixing, sufficient to entrain environmental O_3 in quantities required to convert NO to NO_2 and to maintain a near-environmental concentration of O_3 in the plume for a few minutes, can be reasonably associated with the vortex breakup and decay. The initial turbulent kinetic energy q^2, due to vortex breakup appears to be of the order of one to two m^2/sec^2; only values of q^2 less than the order of 0.1 m^2/sec^2 can be expected to last for 2 to 3 minutes. However, while hydrostatic stability may quickly suppress the vertical component of this turbulence, the lateral component may persist appreciably longer.

As a first, very approximate analysis of the redistribution and chemical alteration of O_3, H_2O, and NO_x, we have assumed that the initial vortex breakup entrains environmental air abruptly, so that there is an initial content of O_3 in the plume, and, following this initial "gulp," the plume is axisymmetric, with the pollutant concentrations, $[H_2O]$ and [NO], distributed in a Gaussian profile with a standard deviation of 10 meters. We further assume that the combination of vertical plume collapse and the rapid damping of any vertical component of turbulence (both of which associate with large hydrostatic stability), produce a "lamina" of plume in the vertical dimension and the pollutant concentrations in this dimension are more or less uniformly distributed within the vertical plume bounds, but retain their essential Gaussian profile in the lateral dimensions initially.

The next step in this analysis is to estimate the total H_2O and NO emitted by an SST per unit distance of travel. For this purpose we have chosen to use a single value of H_2O emission, based on an emission index of 1.3 and a cruise mode fuel consumption rate of 10,000 kg/hr/engine (these estimates seem to be relatively firm). However, the uncertainties in the estimates of NO emissions (as well as a desire to investigate the effects of raising or lowering NO emissions), have led us to choose four values of the NO emission index ranging from 0.010 to .0005. Finally, it was assumed the SST was flying in the sunlit sky, and the photolysis constants were assigned their average daily values.

Six levels of turbulence, ranging from zero to $\overline{v'^2} = 2\ m^2/sec^2$ were run in order to investigate this parameter's influence on plume dilution and chemistry. It was assumed that the chosen level of turbulence was sustained for 200 seconds. All of these estimates and choices led to the nine combinations of input parameters shown in Table 1. In order to facilitate comparison with first-order closure models, we have included the value of effective eddy diffusivity, k_y, which associates with the chosen turbulence fields at $t = 200$ sec. Since, as noted in the explanatory remarks in Table 1, k_y is in fact a function of time during this stage of plume growth, these values of k_y should be used very discreetly.

TABLE 1

Combinations of $[NO]_o$ and $\overline{v'^2}$ chosen for approximate vortex decay simulation. Each of these choices was combined with $[O_3]_o = 4 \times 10^{12}$, $[H_2O]_o = 7.5 \times 10^{16}$, $j_1^* = 1.6 \times 10^{-5}$, $j_1 = 4 \times 10^{-4}$, $j_2 = 10^{-3}$, and $\sigma_y^2 = 100$. (The subscript o denotes a centerline value.)

$\overline{v'^2}$	$[NO]_o$ molecules/cm^3				k_y*
m^2/sec^2	5×10^{12}	10^{13}	5×10^{13}	10^{14}	m^2/sec
0		×			0
0.02		×			1.09
0.10	×	×	×	×	4.46
0.50		×			19.5
1.00		×			35.2
2.00		×			73.0

*k_y is estimated from $k_y = (\sigma_y^2 - \sigma_{y_o}^2)/2t$ at t = 200 sec, where σ_y^2 is the calculated variance of the lateral distributions of $[H_2O]$ and $[NO_x]$, both of which are conservative chemical species in this model. σ_y^2 is, of course, more nearly proportional to t^2 than to t during this period of time, hence k_y is in fact a function of time.

The pertinent results of these simulations of vortex decay mixing and chemistry are listed in Table 2 and displayed in Figs. 15 and 16. In Fig. 15 we examine the dependence of the reactant concentrations on the level of turbulence ($[NO_x]$ is held fixed), and in Fig. 16 we examine the dependence of these plume parameters on the amount of NO_x in the plume ($\overline{v'^2}$ is held fixed). We are particularly interested in the amount of NO converted to NO_2, the concentration of O_3 in the plume, and the concentration of H_2O. Inspection of Fig. 15 shows that, for an initial centerline concentration of NO of 10^{13}, more than half of the NO is converted to NO_2 if $\overline{v'^2}$ is greater than 0.02 m^2/sec^2, and that the O_3 concentrations in the plume are well above 10^{12} molecules/cm^3 for these levels of turbulence. When $\overline{v'^2}$ is in the range of 0.02 to 0.1 m^2/sec^2 the H_2O concentrations are around 10^{16} molecules/cm^3. These results suggest that very modest levels of vortex decay turbulence are capable of setting the stage for HNO_3 formation in the post-vortex phase of the plume life. However, it is also clear that very vigorous turbulence will dilute the H_2O concentrations to values which are marginal for HNO_3 formation.

Turning attention to the effects of varying the NO_x content of the vortex plume, Fig. 16 shows very clearly that a turbulence level of 0.1 m^2/sec^2 is not sufficient to maintain O_3 in the plume when the columnar amount of NO_x exceeds about 10^{21} molecules. Under these circumstances, the NO_x is increasingly dominated by NO (conversion to NO_2 is minimal), and there is an increasing tendency to form an "O_3-hole" in the core of the plume. Since these are realistic ranges for the initial NO content of the SST plume, we are once again reminded that the expected values of NO_x concentrations are in a very critical range for O_3 destruction, a result first suggested by the prior chemistry calculations. However, for our present purposes we simply recognize that the NO_x emission rate is a critical parameter, and choose four initial conditions for the post-vortex chemistry and diffusion calculations. In making these choices we have assumed $\overline{v'^2} = 0.1$ m^2/sec^2 is a reasonable effective value during vortex decay, and have extracted the pertinent initial conditions for post-vortex calculations from the vortex decay simulations for $\overline{v'^2} = 0.1$ m^2/sec^2 and $[NO_x]_I = 1.3 \times 10^{20}$, 2.5×10^{20}, 1.2×10^{21}, and 2.5×10^{21} molecules. All of the pertinent input parameters for post-vortex calculations are shown in Table 3. These choices are hardly exhaustive of all possible conditions; they do tend to bracket reasonable conditions, however, and provide at least a preliminary analysis of the immediate post-vortex chemistry and diffusion of SST exhaust plumes.

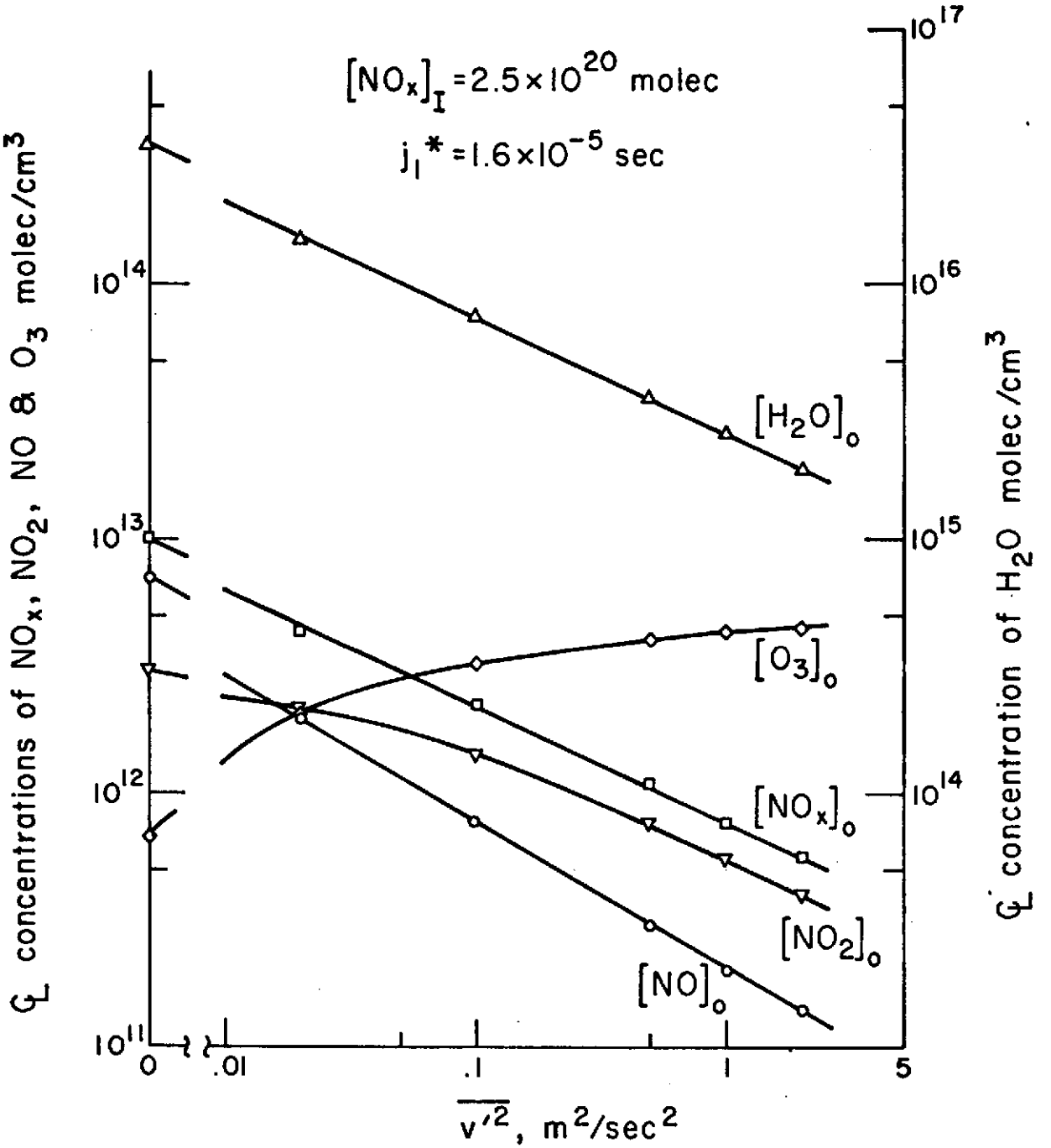

Figure 15. The calculated centerline values of reactant concentrations at 200 sec and as a function of turbulence intensity. Initial conditions are listed in Table 1.

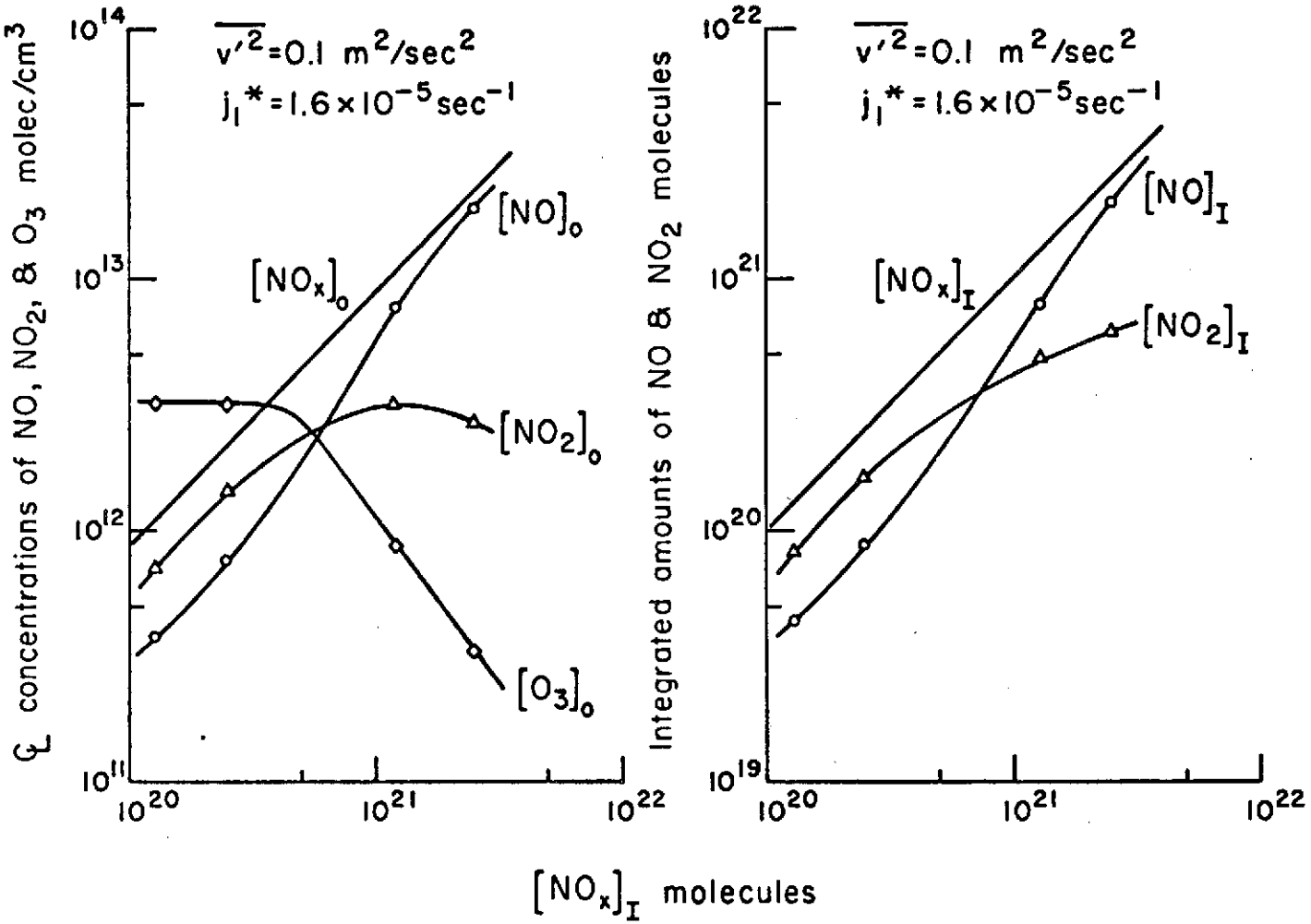

Figure 16a. The calculated initial post-vortex centerline values of $[NO_x]$, [NO], $[NO_2]$ for a fixed value of turbulence and as a function of the total NO_x in a lateral plume column of unit cross-section.

Figure 16b. The calculated initial post-vortex columnar amounts of NO_x, NO, and NO_2.

TABLE 2

Values of plume reactant concentrations and amounts at end of 200 seconds of mixing and chemical reaction. Initially all of the NO_x was NO; other initial conditions are listed in Table 1.

	Integrated Concentrations			Centerline Concentrations		
$\overline{v'^2}$ m^2/sec^2	$[NO_x]_I$	$[NO]_I$	$[NO_2]_I$	$[NO_x]_o$	$[H_2O]_o$	$[O_3]_o$
	molecules			molecules		
.10	1.26×10^{20}	4.4×10^{19}	8.0×10^{19}	1.1×10^{12}	7.6×10^{15}	3.2×10^{12}
0	2.52×10^{20}	1.5×10^{20}	1.0×10^{20}	1.0×10^{13}	3.5×10^{16}	6.7×10^{11}
.02	2.52×10^{20}	1.1×10^{20}	1.4×10^{20}	4.3×10^{12}	1.5×10^{16}	2.1×10^{12}
.10	2.52×10^{20}	8.7×10^{19}	1.6×10^{20}	2.2×10^{12}	7.6×10^{15}	3.2×10^{12}
.50	2.52×10^{20}	7.4×10^{19}	1.8×10^{20}	1.0×10^{12}	3.7×10^{15}	4.1×10^{12}
1.00	2.52×10^{20}	7.1×10^{19}	1.8×10^{20}	7.6×10^{11}	2.6×10^{15}	4.3×10^{12}
2.00	2.52×10^{20}	6.8×10^{19}	1.8×10^{20}	5.4×10^{11}	1.9×10^{15}	4.5×10^{12}
.10	1.26×10^{21}	7.9×10^{20}	4.7×10^{20}	1.1×10^{13}	7.9×10^{15}	8.7×10^{11}
.10	2.52×10^{21}	2.0×10^{21}	5.6×10^{20}	2.2×10^{13}	7.7×10^{15}	3.2×10^{11}

TABLE 3

Initial chemical concentrations and plume dimensions chosen for post-vortex plume chemistry and diffusion calculations.

Item*	Case 1	2	3	4
σ_y^2	1.88×10^3	1.88×10^3	1.83×10^3	1.83×10^3
$[O_3]_o$	3.2×10^{12}	3.2×10^{12}	8.7×10^{11}	3.3×10^{11}
$[H_2O]_o$	7.6×10^{15}	7.6×10^{15}	7.6×10^{15}	7.6×10^{15}
$[NO_x]_o$	1.1×10^{12}	2.2×10^{12}	1.1×10^{13}	2.2×10^{13}
$[NO]_o$	3.8×10^{11}	7.6×10^{11}	7.8×10^{12}	1.9×10^{13}
$[NO_2]_o$	7.0×10^{11}	1.4×10^{12}	3.1×10^{12}	2.7×10^{12}
$[H_2O]_I$	8.8×10^{23}	8.8×10^{23}	8.8×10^{23}	8.8×10^{23}
$[NO_x]_I$	1.3×10^{20}	2.5×10^{20}	1.2×10^{21}	2.5×10^{21}
$[NO]_I$	4.4×10^{19}	8.7×10^{19}	7.9×10^{20}	2.0×10^{21}
$[NO_2]_I$	8.0×10^{19}	1.6×10^{20}	4.7×10^{20}	6.0×10^{19}
$[HNO_3]_I$	9.5×10^{16}	1.9×10^{17}	6.6×10^{17}	1.3×10^{18}

*$[i]_o$ = Plume centerline concentration, molecules/cm^3

$[i]_I$ = Integrated amount across the plume in a column of unit cross-section, molecules.

σ_y^2 = Variance of initial $[H_2O]$ and $[NO_x]$ distributions, m^2.

The environmental values of $[O_3]_e = 5 \times 10^{12}$ molecules/cm^3; all other $[i]_e = 0$.

COUPLED MODEL CALCULATIONS FOR POST-VORTEX CONDITIONS

With the above estimates of the likely range of concentrations and concentration distributions for O_3, NO, NO_2, and H_2O at the end of the vortex decay period, we may proceed to the primary problem of estimating the fate of NO_x and O_3 in the early hours of the post-vortex phase. For these calculations we continue the assumption that diffusive mixing in the vertical dimension is negligible in comparison with lateral diffusion. And, of course, we are interested in a range of lateral turbulence intensities, starting with no turbulence. In addition, since photolysis is an important process in the photochemistry of SST plumes, we have varied the values of j_1^*, j_1, and j_2 for several calculations.

The combinations of $\overline{v'^2}$ and j_1^* used in connection with the four initial concentration distributions listed in Table 3 are shown in Table 4. (j_1 and j_2 were varied in proportion to the variation in j_1^*.) For these initial analyses we have a total of twenty calculations. Each of these calculations was carried out to a real-time simulation of 2.5 hours.

The full computer output for the coupled model comprises an overwhelming mass of information on the state of the system and the rates at which chemical reactions and diffusive processes are going on at each time step for which a print-out is requested. For example, a full concentration profile for each chemical species, the profile of reaction rates for each chemical reaction term in the model, the diffusive flux of each chemical species, and the integrals and higher-order moments of each of the concentration distributions are available at each time step. This detail, of course, permits microscopic examination of any component of the simulation system. Since we are primarily interested in the fate of NO_x and O_3 here, we will forego discussion of these details and concentrate on the distributions of O_3, NO, NO_2, and HNO_3 at the end of 2.5 hrs and as a function of turbulent mixing, photolysis, and the initial conditions for reactant amounts and distributions.

However, as an illustration of the detail with which the processes affecting O_3 and NO_x concentrations are portrayed, we have extracted from one run (at t = 1000 sec) the profiles of the rates at which O_3 and NO are being produced or destroyed by chemistry. These are shown in Fig. 17. Without going into detail, we note that in this particular circumstance the conversion of NO to NO_2 by reaction with O_3 is completely offset by the photolysis of NO_2 and the reaction of NO_2 with O at the core of the plume. In this location NO is being produced, not destroyed, by chemistry. Similar portrayals of the diffusion and other chemical reaction

TABLE 4

Combinations of initial conditions and turbulence chosen for post-vortex plume chemistry and diffusion calculations.

Turbulence	Case							
level	1		2		3		4	
$\overline{v'^2}$	$J_1^*=$	$J_1^*=$	$J_1^*=$	$J_1^*=$	$J_1^*=$	$J_1^*=$	$J_1^*=$	$J_1^*=$
m^2/sec^2	1.6×10^{-5}	8×10^{-5}	1.6×10^{-5}	8×10^{-5}	1.6×10^{-5}	8×10^{-5}	1.6×10^{-5}	8×10^{-5}
0	×	×	×	×	×	×	×	×
.01	×	×	×	×	×	×	×	×
.02	×		×					
.05	×		×					

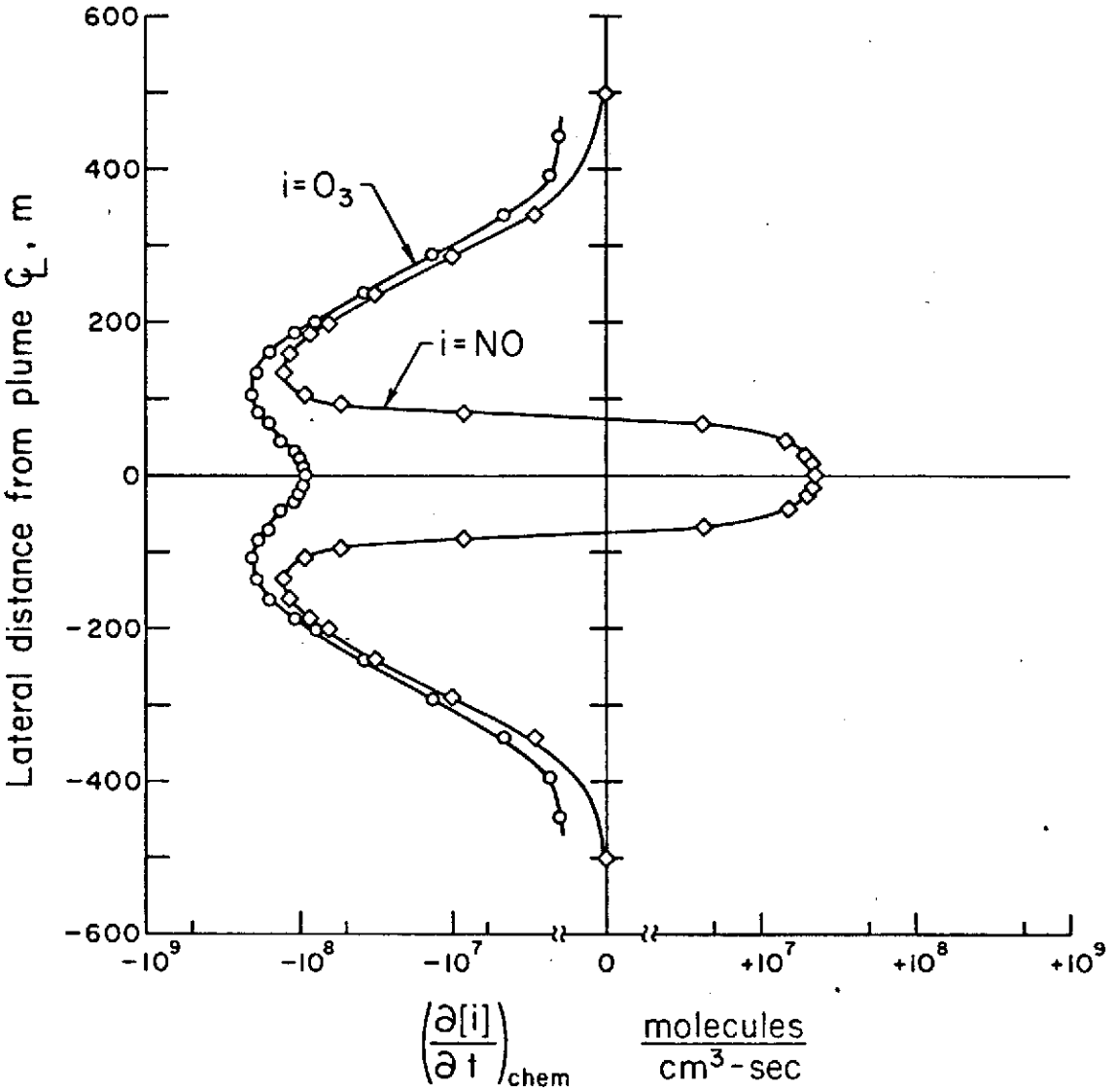

Figure 17. An example of the calculations of the rates at which O_3 and NO are being produced or destroyed as a function of lateral position in the plume.

terms are entirely feasible, if one wishes to pursue such detail. As a first general analysis of the fate of O_3 and NO_x, we shall confine attention to the concentrations of these materials at the centerline of the plume and the integral amount of each chemical species in a lateral column of unit cross-section extending through the plume. From these measures we can readily deduce the production or depletion of each reactant and the dependence of these integral changes on the input conditions.

The Fields of Turbulence in the Lower Stratosphere

Before proceeding to these analyses, it is important to establish the likely levels of lateral turbulent velocities which will operate on the post-vortex plume. Quite literally, the natural small-scale lateral turbulence in the lower stratosphere is unknown. Inferences can be drawn from aircraft measurements of the vertical gust velocities, and, more indirectly, by consideration of the dispersion of materials in this region of the atmosphere (ref. 18). Neither of these are appropriate to the specification of sustained turbulence on the scale of the post-vortex SST plume.

Given this situation, we have chosen to investigate the sensitivity of the fate of O_3 and NO_x to turbulent mixing over a range of turbulence intensities which probably bracket any real circumstance and which, at any rate, go beyond the value of turbulence at which chemical alterations are controlled by diffusive mixing. The need for adequate measurements of stratospheric turbulence, so one can specify where in this range the real processes go on, seems obvious, and is highlighted by the analyses which follow.

As the primary data base for the analyses of the fate of O_3 and NO_x, we have compiled the values of plume width, as measured by the variance of the conservative H_2O distribution, σ_y^2, the plume centerline concentrations of O_3, H_2O, NO_x, NO, and NO_2, designated by $[i]_o$, and the integrated columnar amounts of H_2O, NO_x, NO, NO_2, and HNO_3, designated by $[i]_I$, at t = 2.5 hours and for each of the twenty runs. These are tabulated in Table 5a - f. In addition, the effective eddy difusivities associated with each level of turbulence used and for t = 2.5 hrs are tabulated in Table 6. Finally the calculated deficit of O_3 in the plume, as a fraction of the total O_3 which would occupy the plume column if O_3 were at ambient concentrations, and the deficit of the O_3 plume centerline concentration as a fraction of the ambient O_3 concentration are tabulated for each run in Table 7. Our analyses of coupled chemistry and diffusion in the post-vortex SST plume begins with the data tabulated in Table 6.

TABLE 5a

Plume centerline concentrations, $[i]_o$, variance of $[H_2O]$ $[NO_x]$ lateral distributions, σ_y, and integrated amounts of ith chemical species at $t = 9 \times 10^3$ sec (2.5 hrs), $\overline{v'^2} = 0$, and $j_1^* = 1.6 \times 10^{-5}$ sec^{-1}.

Item*	Case 1	2	3	4
σ_y^2	1.87×10^3	1.86×10^3	1.83×10^3	1.83×10^3
$[O_3]_o$	2.1×10^{12}	9.2×10^{11}	1.2×10^{11}	7.2×10^{10}
$[H_2O]_o$	7.6×10^{15}	7.6×10^{15}	7.7×10^{15}	7.7×10^{15}
$[NO_x]_o$	1.1×10^{12}	2.2×10^{12}	1.1×10^{13}	2.2×10^{13}
$[NO]_o$	4.6×10^{11}	1.4×10^{12}	1.0×10^{13}	2.1×10^{13}
$[NO_2]_o$	6.0×10^{11}	7.8×10^{11}	7.9×10^{11}	9.6×10^{11}
$[H_2O]_I$	8.8×10^{23}	8.8×10^{23}	8.8×10^{23}	8.8×10^{23}
$[NO_x]_I$	1.3×10^{20}	2.5×10^{20}	1.2×10^{21}	2.5×10^{21}
$[NO]_I$	4.6×10^{19}	1.3×10^{20}	1.1×10^{21}	2.3×10^{21}
$[NO_2]_I$	7.7×10^{19}	1.2×10^{20}	1.6×10^{20}	2.0×10^{20}
$[HNO_3]_I$	2.9×10^{18}	2.3×10^{18}	1.1×10^{18}	1.5×10^{18}

*$[i]_o$ = Plume centerline concentration, molecules/cm^3

$[i]_I$ = Integrated amount across the plume in a column of unit cross-section, molecules.

σ_y^2 = Variance of $[H_2O]$ and $[NO_x]$, m^2.

The environmental values of $[O_3]_e = 5 \times 10^{12}$ molecules/cm^3; all other $[i]_e = 0$.

TABLE 5b

Same as Table 5a, except $\overline{v'^2} = 0$ m^2/sec^2 and $j_1^* = 8 \times 10^{-5}$ sec^{-1}.

Item*	Case 1	2	3	4
σ_y^2	1.87×10^3	1.87×10^3	1.83×10^3	1.83×10^3
$[O_3]_o$	2.3×10^{12}	1.3×10^{12}	3.1×10^{11}	2.5×10^{11}
$[H_2O]_o$	7.6×10^{15}	7.6×10^{15}	7.7×10^{15}	7.7×10^{15}
$[NO_x]_o$	1.1×10^{12}	2.2×10^{12}	1.1×10^{13}	2.2×10^{13}
$[NO]_o$	7.6×10^{11}	1.8×10^{12}	1.0×10^{13}	2.1×10^{13}
$[NO_2]_o$	2.2×10^{11}	3.0×10^{11}	7.7×10^{11}	6.8×10^{12}
$[H_2O]_I$	8.8×10^{23}	8.8×10^{23}	8.8×10^{23}	8.8×10^{23}
$[NO_x]_I$	1.2×10^{20}	2.5×10^{20}	1.2×10^{21}	2.5×10^{21}
$[NO]_I$	8.3×10^{19}	1.9×10^{20}	1.2×10^{21}	2.4×10^{21}
$[NO_2]_I$	2.9×10^{19}	4.7×10^{19}	7.7×10^{19}	1.2×10^{20}
$[HNO_3]_I$	1.4×10^{19}	1.2×10^{19}	3.8×10^{18}	3.1×10^{18}

*$[i]_o$ = Plume centerline concentration, molecules/cm^3

$[i]_I$ = Integrated amount across the plume in a column of unit cross-section, molecules.

σ_y^2 = Variance of $[H_2O]$ and $[NO_x]$, m^2.

The environmental values of $[O_3]_e = 5 \times 10^{12}$ molecules/cm^3; all other $[i]_e = 0$.

TABLE 5c

Same as Table 5a, except $\overline{v'^2}$ = 0.01 m^2/sec^2 and j_1^* = 1.6 × 10^{-5} sec^{-1}.

Item*	Case 1	2	3	4
σ_y^2	3.1 × 10^5	3.1 × 10^5	3.0 × 10^5	3.0 × 10^5
$[O_3]_o$	4.8 × 10^{12}	4.7 × 10^{12}	9.3 × 10^{11}	1.5 × 10^{12}
$[H_2O]_o$	6.0 × 10^{14}	6.0 × 10^{14}	6.0 × 10^{14}	5.9 × 10^{14}
$[NO_x]_o$	8.6 × 10^{10}	1.7 × 10^{11}	8.5 × 10^{11}	1.7 × 10^{12}
$[NO]_o$	2.1 × 10^{10}	4.3 × 10^{10}	5.3 × 10^{11}	8.8 × 10^{11}
$[NO_2]_o$	6.2 × 10^{10}	1.2 × 10^{10}	3.2 × 10^{11}	8.1 × 10^{11}
$[H_2O]_I$	8.8 × 10^{23}	8.8 × 10^{23}	8.8 × 10^{23}	8.8 × 10^{23}
$[NO_x]_I$	1.3 × 10^{20}	2.5 × 10^{20}	1.3 × 10^{21}	2.5 × 10^{21}
$[NO]_I$	3.1 × 10^{19}	6.4 × 10^{19}	4.5 × 10^{20}	1.1 × 10^{21}
$[NO_2]_I$	9.2 × 10^{19}	1.9 × 10^{20}	8.0 × 10^{20}	1.4 × 10^{21}
$[HNO_3]_I$	4.1 × 10^{18}	4.2 × 10^{18}	3.1 × 10^{18}	2.8 × 10^{18}

*$[i]_o$ = Plume centerline concentration, molecules/cm^3

$[i]_I$ = Integrated amount across the plume in a column of unit cross-section, molecules.

σ_y^2 = Variance of $[H_2O]$ and $[NO_x]$, m^2.

The environmental values of $[O_3]_e$ = 5 × 10^{12} molecules/cm^3; all other $[i]_e$ = 0.

TABLE 5d

Same as Table 5a, except $\overline{v'^2}$ = 0.01 m^2/sec^2 and j_1^* = 8 × 10^{-5} sec^{-1}.

Item*	Case 1	2	3	4
σ_y^2	3.4 × 10^5	3.2 × 10^5	3.0 × 10^5	2.7 × 10^5
$[O_3]_o$	4.7 × 10^{12}	4.6 × 10^{12}	2.8 × 10^{12}	1.3 × 10^{12}
$[H_2O]_o$	6.0 × 10^{14}	6.0 × 10^{14}	6.0 × 10^{14}	6.4 × 10^{14}
$[NO_x]_o$	8.6 × 10^{10}	1.7 × 10^{11}	8.5 × 10^{11}	1.8 × 10^{12}
$[NO]_o$	4.4 × 10^{10}	9.9 × 10^{10}	6.2 × 10^{11}	1.6 × 10^{12}
$[NO_2]_o$	2.6 × 10^{10}	5.7 × 10^{10}	2.2 × 10^{11}	2.5 × 10^{11}
$[H_2O]_I$	8.9 × 10^{23}	8.9 × 10^{23}	8.8 × 10^{23}	8.8 × 10^{23}
$[NO_x]_I$	1.3 × 10^{20}	2.5 × 10^{20}	1.3 × 10^{21}	2.5 × 10^{21}
$[NO]_I$	6.8 × 10^{19}	1.5 × 10^{20}	8.8 × 10^{20}	2.0 × 10^{21}
$[NO_2]_I$	4.0 × 10^{19}	8.6 × 10^{19}	3.7 × 10^{20}	5.4 × 10^{20}
$[HNO_3]_I$	2.1 × 10^{19}	2.0 × 10^{19}	1.4 × 10^{19}	8.7 × 10^{18}

*$[i]_o$ = Plume centerline concentration, molecules/cm^3

$[i]_I$ = Integrated amount across the plume in a column of unit cross-section, molecules.

σ_y^2 = Variance of $[H_2O]$ and $[NO_x]$, m^2.

The environmental values of $[O_3]_e$ = 5 × 10^{12} molecules/cm^3; all other $[i]_e$ = 0.

TABLE 5e

Same as Table 5a, except $\overline{v'^2} = 0.02\ m^2/sec^2$ and $j_1^* = 1.6 \times 10^{-5}\ sec^{-1}$

	Case			
Item*	1	2	3	4
σ_y^2	6.1×10^5	5.9×10^5		
$[O_3]_o$	4.8×10^{12}	4.8×10^{12}	N	N
$[H_2O]_o$	4.3×10^{14}	4.3×10^{14}	O	O
$[NO_x]_o$	6.2×10^{10}	1.2×10^{11}	T	T
$[NO]_o$	1.5×10^{10}	3.0×10^{10}		
$[NO_2]_o$	4.5×10^{10}	9.0×10^{10}		
$[H_2O]_I$	8.8×10^{23}	8.9×10^{23}	R	R
$[NO_x]_I$	1.3×10^{20}	2.5×10^{20}	U	U
$[NO]_I$	3.0×10^{19}	6.2×10^{19}	N	N
$[NO_2]_I$	9.2×10^{19}	1.9×10^{20}		
$[HNO_3]_I$	4.2×10^{18}	4.2×10^{18}		

*$[i]_o$ = Plume centerline concentration, molecules/cm^3

$[i]_I$ = Integrated amount across the plume in a column of unit cross-section, molecules.

σ_y^2 = Variance of $[H_2O]$ and $[NO_x]$, m^2.

The environmental values of $[O_3]_e = 5 \times 10^{12}$ molecules/cm^3; all other $[i]_e = 0$.

TABLE 5f

Same as Table 5a, except $\overline{v'^2}$ = 0.05 m^2/sec^2 and j_1^* = 1.6 × 10^{-5} sec^{-1}.

Item*	Case 1	2	3	4
σ_y^2	1.5 × 10^6	1.4 × 10^6		
$[O_3]_o$	4.9 × 10^{12}	4.9 × 10^{12}	N	N
$[H_2O]_o$	2.8 × 10^{14}	2.8 × 10^{14}	O	O
$[NO_x]_o$	4.0 × 10^{10}	7.9 × 10^{10}	T	T
$[NO]_o$	9.3 × 10^9	1.9 × 10^{10}		
$[NO_2]_o$	2.9 × 10^{10}	5.8 × 10^{10}		
$[H_2O]_I$	8.9 × 10^{23}	8.9 × 10^{23}	R	R
$[NO_x]_I$	1.3 × 10^{20}	2.5 × 10^{20}	U	U
$[NO]_I$	3.0 × 10^{19}	6.2 × 10^{19}	N	N
$[NO_2]_I$	9.2 × 10^{19}	1.9 × 10^{20}		
$[HNO_3]_I$	4.3 × 10^{18}	4.4 × 10^{18}		

*$[i]_o$ = Plume centerline concentration, molecules/cm^3

$[i]_I$ = Integrated amount across the plume in a column of unit cross-section, molecules.

σ_y^2 = Variance of $[H_2O]$ and $[NO_x]$, m^2.

The environmental values of $[O_3]_e$ = 5 × 10^{12} molecules/cm^3; all other $[i]_e$ = 0.

TABLE 6

The effective eddy diffusivity, k_y, associated with turbulence levels chosen for post-vortex plume chemistry and diffusion calculations, based on $\sigma_y^2 = 2kt$ at $t = 2.5$ hrs.

Turbulence level $\overline{v'^2}$ (m^2/sec^2)	Effective Eddy Diffusivity, k_y (m^2/sec)
0	0
0.01	1.7×10^1
0.02	3.2×10^1
0.05	8.2×10^1

TABLE 7

The fractional deficit of O_3 in a plume column, a, and at the plume centerline, b, as a function of the columnar NO_x, $[NO_x]_I$, the turbulence $\overline{v'^2}$, and the photolysis rate, j_1^*.

		$[NO_x]_I$ Molecules							
	O_3	1.26×10^{20}		2.52×10^{20}		1.26×10^{21}		2.52×10^{21}	
$\overline{v'^2}$ m^2/sec^2	Def.	j_1^* = 1.6×10^{-5}	8×10^{-5}	1.6×10^{-5}	8×10^{-5}	1.6×10^{-5}	8×10^{-5}	1.6×10^{-5}	8×10^{-5}
0	a	.140	.148	.210	.200	.38	.38	.40	.37
	b	.58	.54	.82	.74	.98	.98	.98	.95
0.01	a	.010	.008	.015	.017	.082	.094	.165	.090
	b	.04	.06	.06	.08	.81	.44	.70	.74
0.02	a	.008		.012					
	b	.04		.04					
0.05	a	.005		.006					
	b	.02		.02					

The Fate of O_3 in the Post-Vortex Plume

The fate of O_3 during the first few hours of the SST plume life is of interest for two reasons; 1) the concentration of O_3 in the plume determines the production of $O(^1D)$ in the sunlit sky, and, therefore, the production of OH and, subsequently, HNO_3; 2) if the O_3 is seriously depleted in the plume, the catalytic destruction of O_3 by the NO_x cycle is much reduced (ref. 4). Depending upon how long this latter situation persists, the O_3 depletion may alter the estimate of the efficiency of the NO_x catalytic cycle in the general problem of environmental impact.

In the first problem, i.e., the O_3 role in HNO_3 production, we must also be concerned about the depletion of O_3 in relation to the profiles of H_2O and NO_2. Since $[H_2O]$ is a maximum at the plume centerline, and $[NO_2]$ tends to be concentrated in the plume core (where $[NO_x]$ is a maximum), we have examined the plume centerline depletion of O_3, as well as the columnar depletion across the plume.

An inspection of Table 7 points up quickly under what circumstances the depletion of O_3 becomes significant. The maximum depletion of O_3 associates, not surprisingly, with minimum turbulent mixing (O_3 is not entrained from the environment), and with maximum values of NO_x. However, in the sunlit sky, the regenerative capacity for the production of O_3 in the plume is sufficient to limit the columnar depletion of O_3 to about 40 to 50 per cent, although the centerline concentration of O_3 has essentially gone to zero when $[NO_x]_I$ exceeds 3×10^{21} molecules. (The importance of this O_3 depletion to HNO_3 formation is discussed in the next section.) The general depletion of O_3 in the plume appears to become significant when the turbulence level is less than 0.01 m^2/sec^2 and the $[NO_x]_I$ exceeds 1.26×10^{21} molecules. The latter number associates with an emission index for NO_x of about 0.005, which is only about 1/40th current NO_x emission control technology (ref. 19). Since near-zero levels of small-scale turbulence may also be more the rule than the exception in the lower stratosphere, we conclude that the early depletion of O_3 in the SST plume cannot be dismissed out of hand.

Within the ranges of the input variables tested, the data in Table 7 permit an "engineering" estimate of the relationships between O_3 depletion and the controlling variables, $\overline{v'^2}$ and $[NO_x]_I$. First, a plot of plume centerline O_3 deficit, $\Delta O_3(\text{CL})$, vs the columnar deficit, $\Delta O_3(\text{Col})$, (Fig. 18) shows these quantities are highly correlated for all values of $\overline{v'^2}$ and $[NO_x]_I$ tested. This

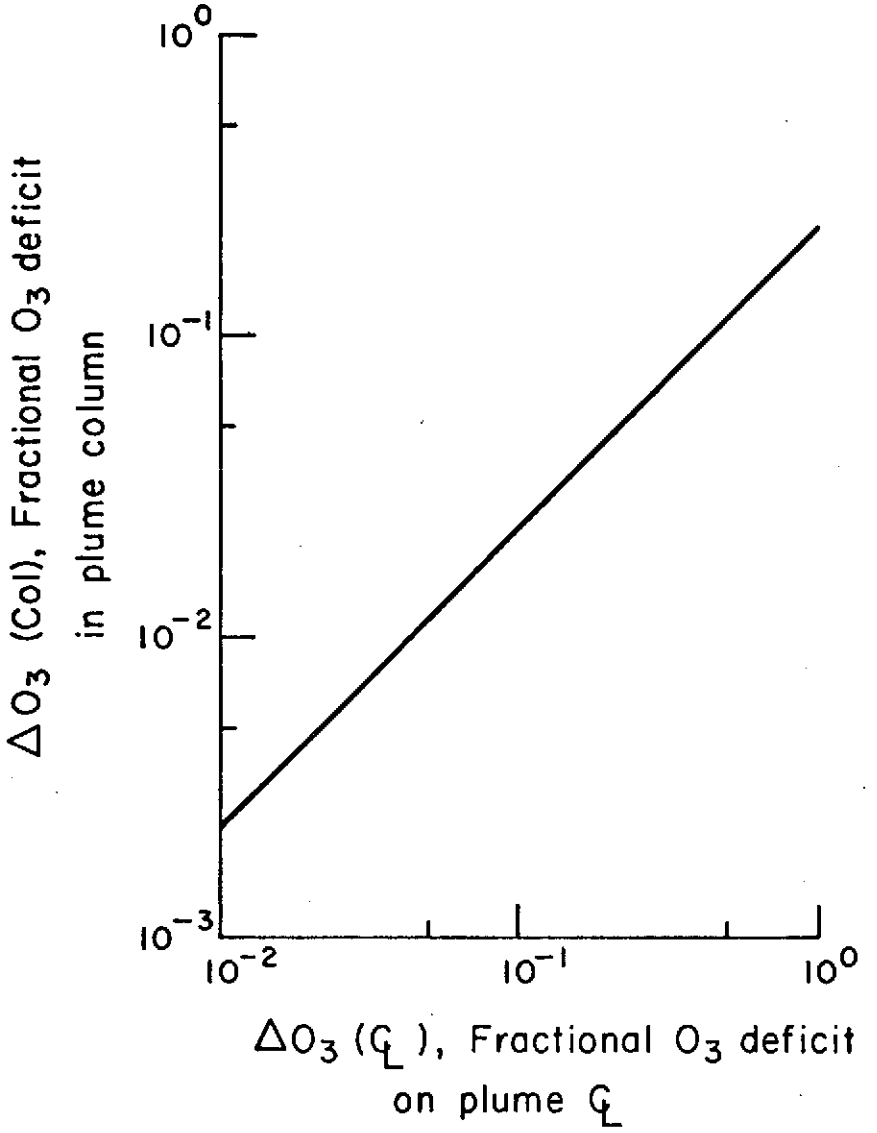

Figure 18. The relationship of O_3 deficits at the plume centerline to the columnar O_3 deficit at t = 2.5 hrs.

result suggests that, for this wide variety of conditions, the O_3 concentration profiles have a high degree of self-similarity. Within the ranges tested,

$$\frac{\Delta O_3(G_L)}{\Delta O_3(\text{Col})} = 4 \tag{66}$$

The partial dependence of $\Delta O_3(G_L)$ on $[NO_x]_I$ and $\overline{v'^2}$ is shown in Fig. 19. These data yield the relationship,

$$\Delta O_3(G_L) = C_1 \frac{[NO_x]_I}{(\overline{v'^2})^{\frac{1}{2}}} \begin{cases} (\overline{v'^2} > .001) \\ ([NO_x]_I < 2.5 \times 10^{21}) \end{cases} \tag{67}$$

where $C_1 \tilde{=} 3 \times 10^{-23}$. Since the chemistry calculations have shown that $[O_3]$ is insensitive to $[H_2O]$ until $[H_2O]$ exceeds 10^{17} molecules/cm^3 (an excessive value in the post-vortex plume), Eq. (67) captures the essential dependence of the plume O_3 deficit on plume and turbulence parameters. We note in particular that a significant O_3-hole develops at the core of the plume when the ratio $[NO_x]_I/(\overline{v'^2})^{\frac{1}{2}}$ exceeds 3×10^{22}, a value only slightly beyond the range we have tested.

The Fate of NO_x in the Post-Vortex Plume

In examining the predicted fate of NO_x in the early post-vortex plume, we are primarily interested in the rapid formation of HNO_3. This interest, of course, resides in the strong buffering of the NO_x catalytic cycle for the destruction of O_3 which conversion to HNO_3 represents. The chemistry calculations have shown this conversion is rapid only when high concentrations of H_2O and O_3 are associated with significant concentrations of NO_2. If this conversion of NO_2 to HNO_3 is to be a significant factor in the SST problem, it must occur before the H_2O is diluted by turbulent mixing. These early plume calculations are, therefore, particularly pertinent to this phase of the problem.

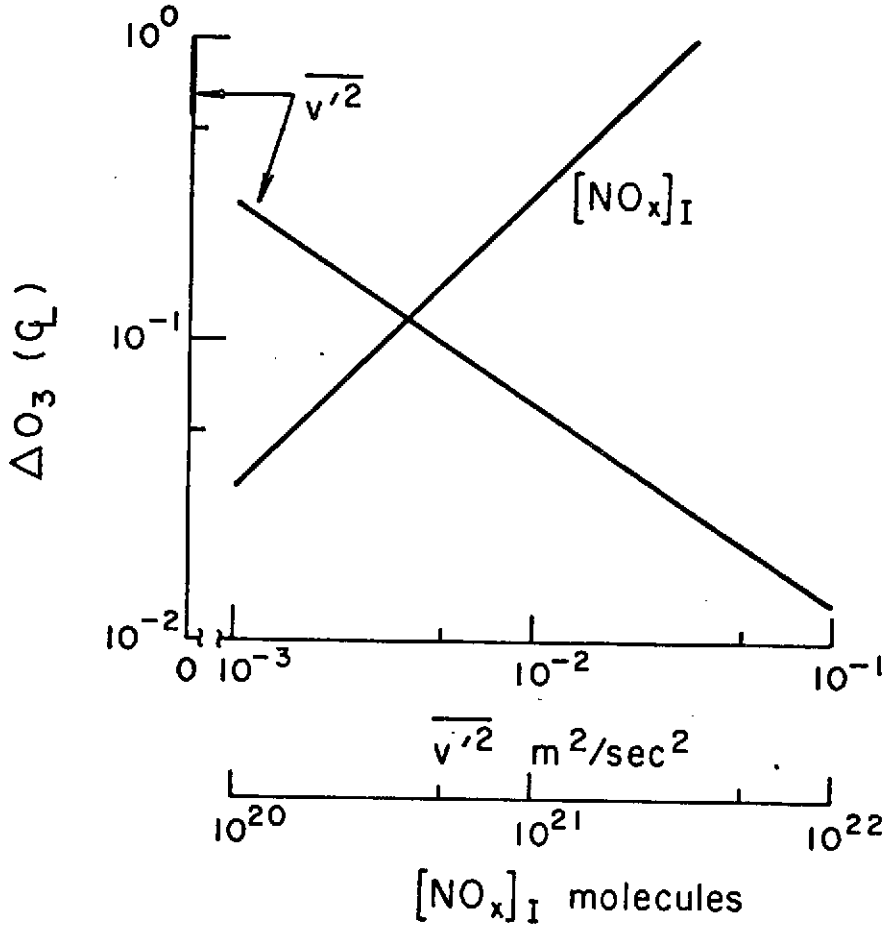

Figure 19. The partial dependence of the O_3 centerline deficit at 2.5 hrs on 1) the level of turbulence, $\overline{v'^2}$, and 2) the amount of NO_x in the plume, $[NO_x]_I$.

The results of the model calculations of HNO_3 formation during 2.5 hrs and for the various conditions listed in Tables 3 and 4 are tabulated in Tables 8 and 9 and displayed graphically in Fig. 20. Inspection of either of these displays reveals very quickly that the fraction of NO_x converted to HNO_3 is greater than 10 per cent only for minimum values of $[NO_x]_I$ and maximum values of j_1^*. If the conditions tested are at all representative of the SST post-vortex plume, the early formation of HNO_3 cannot be reckoned as a significant process. This conclusion would be modified for cases where j_1^* and $[H_2O]$ are somewhat higher than the limits used here, i.e., higher in the stratosphere and for engines with larger fuel consumption rates. But, for the present problem, it appears early HNO_3 formation provides only a minor safeguard against the later catalytic destruction of O_3 by NO and NO_2.

It is interesting to note that the formation of HNO_3 is enhanced by turbulent mixing. The reason for this behavior is, of course, ascribable to the fact that the entrainment of environmental O_3 more than offsets the dilution of the other reactants. This general interplay among $\overline{v'^2}$, O_3, and NO_x in the formation of HNO_3 can be seen when we plot the columnar O_3 deficit against $[HNO_3]_I/[NO_x]_I$, as shown in Fig. 21. This figure only identifies the inverse association of the O_3 deficit with the suppression of HNO_3 formation as a function of the turbulent mixing. However, this comparison points up the mutual fates of NO_x and O_3, namely, when O_3 is depleted, due mainly to increasing NO_x concentrations, the formation of HNO_3 is suppressed. Although HNO_3 formation does not now appear significant, we may note in passing that any reduction in NO emissions not only reduces the total NO_x in the stratosphere, but also leads to a larger fraction of the NO_x being converted early-on to HNO_3. It remains to be seen as to whether this compounding effect of NO_x reduction produces a significant change in NO-NO_2 concentrations, and therefore in O_3 destruction, at useful operational limits.

CONCLUSIONS

The final evaluation and interpretation of these simulations of chemistry and diffusion in highly perturbed stratospheres must be deferred until validation data regarding the turbulence fields and the chemical composition of the early SST exhaust plume have been obtained experimentally. This final proof of any simulation model becomes particularly important in this case because of the unusual sensitivity of the fates of O_3 and NO_x to the amount of NO_x

TABLE 8

The total formation of HNO_3 in 2.5 hrs for various initial conditions and turbulence levels, $[HNO_3]_I$ in 10^{18} molecules.

Turbulence level	$[NO_x]_I$ Molecules							
	1.26×10^{20}		2.52×10^{20}		1.26×10^{21}		2.52×10^{21}	
$\overline{v'^2}$ m^2/sec^2	$j_1^* =$ 1.6×10^{-5}	8×10^{-5}	1.6×10^{-5}	8×10^{-5}	1.6×10^{-5}	8×10^{-5}	1.6×10^{-5}	8×10^{-5}
0	2.87	14.4	2.33	11.8	1.08	1.08	1.49	3.1
.01	4.13	20.6	4.16	20.3	3.10	14.0	2.73	8.7
.02	4.20		4.26					
.05	4.30		4.35					

TABLE 9

The fraction of NO_x converted to HNO_3 in 2.5 hrs.

	$[NO_x]_I$ Molecules							
Turbulence level	1.26×10^{20}		2.52×10^{20}		1.26×10^{21}		2.52×10^{21}	
$\overline{v'^2}$ m^2/sec^2	$j_1^* =$ 1.6×10^{-5}	8×10^{-5}	1.6×10^{-5}	8×10^{-5}	1.6×10^{-5}	8×10^{-5}	1.6×10^{-5}	8×10^{-5}
0	.023	.114	.009	.047	<.001	.001	<.001	.001
.01	.035	.164	.016	.081	.002	.011	.001	.004
.02	.033		.017					
.05	.034		.017					

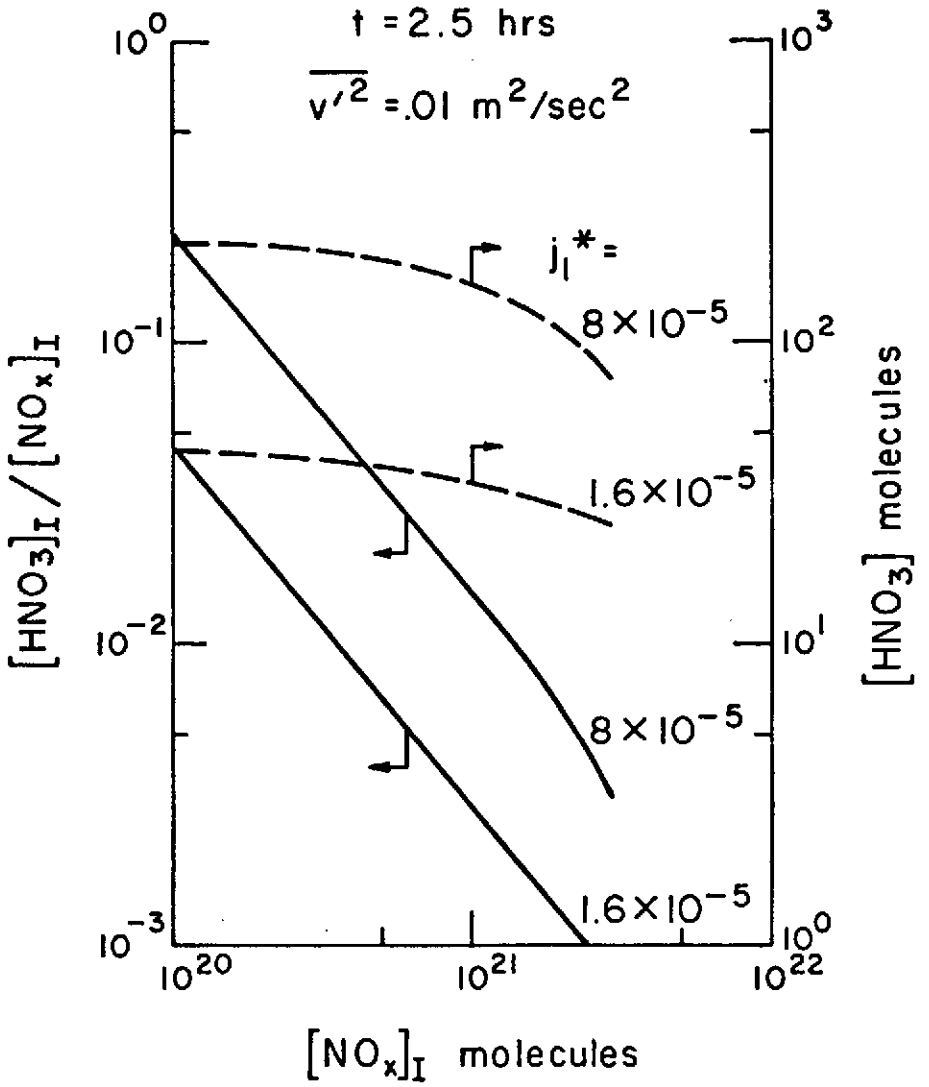

Figure 20. The dependence of fractional conversion of NO_x to HNO_3 during 2.5 hours on the amount of NO_x in the plume and two values of the photolysis constants.

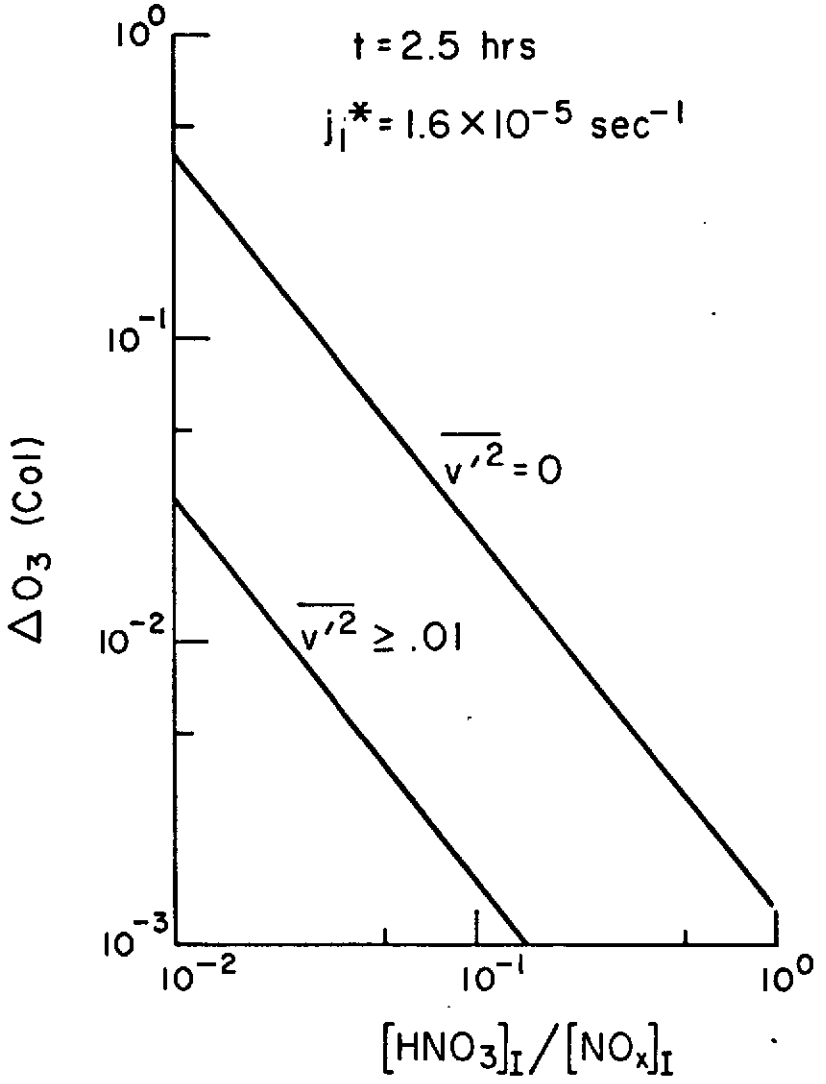

Figure 21. Joint values of plume O_3 depletion and HNO_3 formation in 2.5 hours as calculated by the coupled diffusion/chemistry model.

in the plume. Best estimates of this quantity now place the NO_x emissions and initial plume NO_x concentrations precisely in this range of greatest sensitivity, i.e., 10^{12} to 10^{14} molecules/cm^3 in the core of the post-vortex plume, and generally in the range 10^{10} to 10^{12} in the other parts of the plume. The remarkable decline of O_3 concentrations as the NO_x concentrations go above 10^{12} molecules/cm^3 poses a "continental divide" effect insofar as the fates of O_3 and HNO_3 formation in the plume are concerned. When NO_x concentrations go above 10^{12} molecules/cm^3, O_3 concentrations are rapidly suppressed, and HNO_3 formation is inhibited due to the lack of O('D). When $[NO_x]$ exceeds 10^{13} the destruction of O_3 is essentially complete, resulting in an "O_3-hole" in that region (generally the core) of the plume. The importance of this O_3 deficit to other chemical reactions, such as the fate of unburned hydrocarbons, has not been investigated in the present study.

When $[NO_x] < 10^{12}$ molecules/cm^3, O_3 is only very slowly depleted and, given H_2O concentrations above 10^{14} to 10^{15} molecules/cm^3, the formation of HNO_3 is predicted. However, on the basis of plume conditions examined here, significant conversion of NO_x to HNO_3 in a time period of a few hours occurs only when $[H_2O]$ is present in excess of about 10^{16} molecules/cm^3 and $[NO_x]$ is less than 10^{11} molecules/cm^3. These are incompatible requirements for present H_2O and NO_x emission estimates, since they require a minimum dilution of NO_x of about two to three orders of magnitude, but a maximum dilution of H_2O of only ten. Since H_2O and NO_x emanate from a common source, differential dilution of these exhaust constituents in the ratio of one to two orders of magnitude is not physically possible. On this basis, we conclude that significant HNO_3 formation in the first few hours of plume life is not likely under the emission estimates presently used for H_2O and NO_x.

We do note, however, that these simulations provide a basis for estimating the change in the environmental impact of reducing SST NO_x emissions which go beyond the simple proportional reduction in NO and NO_2. If the initial post-vortex concentrations of NO_x are reduced below 10^{12} molecules/cm^3 by emission controls, but the H_2O concentrations remain in the 10^{16} molecules/cm^3 range, then, in the sunlit sky, a significant fraction of the NO_x can be converted to HNO_3 within a few hours. Since the photolysis of HNO_3, to recover NO_2 and OH, is slow, this conversion, if realized, would effectively buffer the NO-NO_2 catalytic cycle for the destruction of O_3. Just where these compounding effects of proportional reduction of $[NO]$ and $[NO_2]$ by emissions controls and HNO_3 formation sets in

depends upon reliable estimates of NO_x emission rates and turbulent mixing in the post-vortex plume. But, the simulation models for evaluating the payoff of NO_x emission controls in decreased destruction of O_3 are available.

Finally, the role of stratospheric turbulence in the determination of the fates of O_3 and HNO_3 are now much clearer. The primary roles of turbulent mixing are 1) to entrain environmental O_3 into the post-vortex plume, and 2) to dilute the NO_x and H_2O concentrations in the plume, and, of course, to spread these exhaust constituents through an increasing volume of the stratosphere. We have argued that near-zero values of small-scale atmospheric turbulence should be quite common, indeed, the rule in the lower stratosphere. Under these circumstances the mixing of exhaust materials with the environmental O_3, and the dilution of exhaust constituents are both very slow, and the chemical fate of exhaust materials is controlled by their relative abundance within the plume. During the time this nonturbulent condition persists, plume segments remain more or less intact (they may be distorted but not diluted by larger scale wind shear), and the internal balances of $[O_3]$, [NO], $[NO_2]$, and $[HNO_3]$ operate on a "do-nothing" cycle. This very real possibility becomes significant to the environmental impact assessment of SST operations when these intact plume segments persist for a significant fraction of the residence time of exhaust materials in the lower stratosphere.

At this point the lack of hard data on the turbulence history of individual small volumes of air in the lower stratosphere precludes a definitive assessment of this effect. What is needed are measurements of the time history of turbulence in the vicinity of free-floating balloons which track these individual volumes of air as they circumnavigate the globe. With appropriate turbulence instrumentation (the primary requirements are for resolution of vertical and lateral gusts down to rms values of the order 2-5 cm/sec), the basic problems of turbulent mixing, the sporadic nature of this mixing, and the recurrence period for significant turbulence could be resolved. These data would permit much more realistic and reliable estimates of the fates of SST exhaust materials and of environmental O_3 than are now available.

The problem of the residence time of SST exhaust materials in the lower stratosphere, given the highly specialized altitude and geographical locations of the SST flight routes, goes beyond the immediate purposes of the present study somewhat, but is repeated here for emphasis in interpreting the significance of early plume chemistry and diffusion. The validity of the assumption of a laterally well-mixed lower stratosphere, in which the contribution of SST exhausts are treated as a fractional perturbation of the background values of NO_x and H_2O, hinges on a reliable estimate of this residence time.

ACKNOWLEDGMENTS

The substantial program of model development and operations summarized here are the results of contributions and dedicated effort by several people. The contributions of Dr. Milton Teske and Mr. Ross Contiliano, who programmed these models for computer solutions, and of Dr. Johnny Freiberg, who sorted out the photochemistry, were particularly important and are gratefully acknowledged. A special note of gratitude is due Dr. Coleman duP. Donaldson for his continued interest and support in these studies, and for the very fundamental developments upon which these models are based.

APPENDIX A

The Effect of Incomplete Mixing During Vortex Decay on the Conversion of NO to NO_2

We examine the effect of neglecting the mixedness term in the vortex decay calculations. Since the primary reaction of interest during the vortex decay period is the conversion of NO to NO_2 by O_3, we can examine this effect by using an earlier version of the coupled model in which H_2O was neglected, but the term $\overline{[O_3]'[NO]'}$ was retained in the calculation (ref. 5). In this case the mean time rate of change of [NO] is given by

$$\frac{d[\overline{NO}]}{dt} = -\frac{\partial}{\partial y}\overline{v'[NO]'} - k_2([\overline{NO}][\overline{O}_3] + \overline{[NO]'[O_3]'}) + j_2[\overline{NO}_2] \quad (A1)$$

Then

$$\int_{-\infty}^{\infty}\frac{d[\overline{NO}]}{dt}\,dy = -\int_{-\infty}^{\infty}\frac{\partial}{\partial y}\overline{v'[NO]'}\,dy - k_2\int_{-\infty}^{\infty}([\overline{NO}][\overline{O}_2] + \overline{[NO]'[O_3]'})\,dy$$

$$+ j_2\int_{-\infty}^{\infty}[\overline{NO}_2]\,dy \quad (A2)$$

But

$$\int_{-\infty}^{\infty}\frac{d[\overline{NO}]}{dt}\,dy = \frac{d}{dt}\int_{-\infty}^{\infty}[\overline{NO}]\,dy = \frac{d[NO]_I}{dt} \quad (A3)$$

$$\int_{-\infty}^{\infty} \frac{\partial}{\partial y} v'[\overline{NO}]' \, dy = 0 \tag{A4}$$

and

$$j_2 \int_{-\infty}^{\infty} [\overline{NO_2}] \, dy = j_2[\overline{NO_2}]_I \tag{A5}$$

Then

$$\frac{d[\overline{NO}]_I}{dt} = - k_2 \int_{-\infty}^{\infty} ([\overline{NO}][\overline{O_3}] + \overline{[NO]'[O_3]'}) \, dy + j_2[\overline{NO_2}]_I \tag{A6}$$

If the mixedness term $\overline{[NO]'[O_3]'}$ is set equal to zero,

$$\frac{d[NO]_I^*}{dt} = - k_2 \int_{-\infty}^{\infty} [\overline{NO}][\overline{O_3}] \, dy + j_2[\overline{NO_2}]_I \tag{A7}$$

and

$$\frac{d[\overline{NO}]_I/dt - j_2[\overline{NO}]_I}{d[\overline{NO}]_I^*/dt - j_2[\overline{NO}]_I} = \frac{[[\overline{NO}][\overline{O_3}] + \overline{[NO]'[O_3]'}]_I}{[[\overline{NO}][\overline{O_3}]]_I} \tag{A8}$$

To estimate the magnitude of the term on the right-hand side of Eq. (A8), this model was run for the vortex decay case, $\overline{v'^2}$ = 0.1 m^2/sec^2, $[O_3]_o = 4 \times 10^{12}$ molecules/cm^3, $[NO]_o = 10^{13}$ molecules/cm^3, $[NO_2] = 0$, and $\sigma_{yo}^2 = 100$ m^2. The values of $[\overline{[NO]'[O_3]'}]_I/([\overline{NO}][\overline{O_3}])_I$ for 400 seconds are shown in Fig. A-1. As can be seen there, the effect of mixedness is to suppress the reaction between $[O_3]$ and [NO]. This effect reaches a maximum of about 30 per cent around 75 seconds and has decayed to less than 10 per cent after 300 seconds. On this basis the coupled model used in the present study overestimates the conversion of NO to NO_2 by approximately 20 per cent during the 200 seconds assumed for vortex decay turbulence.

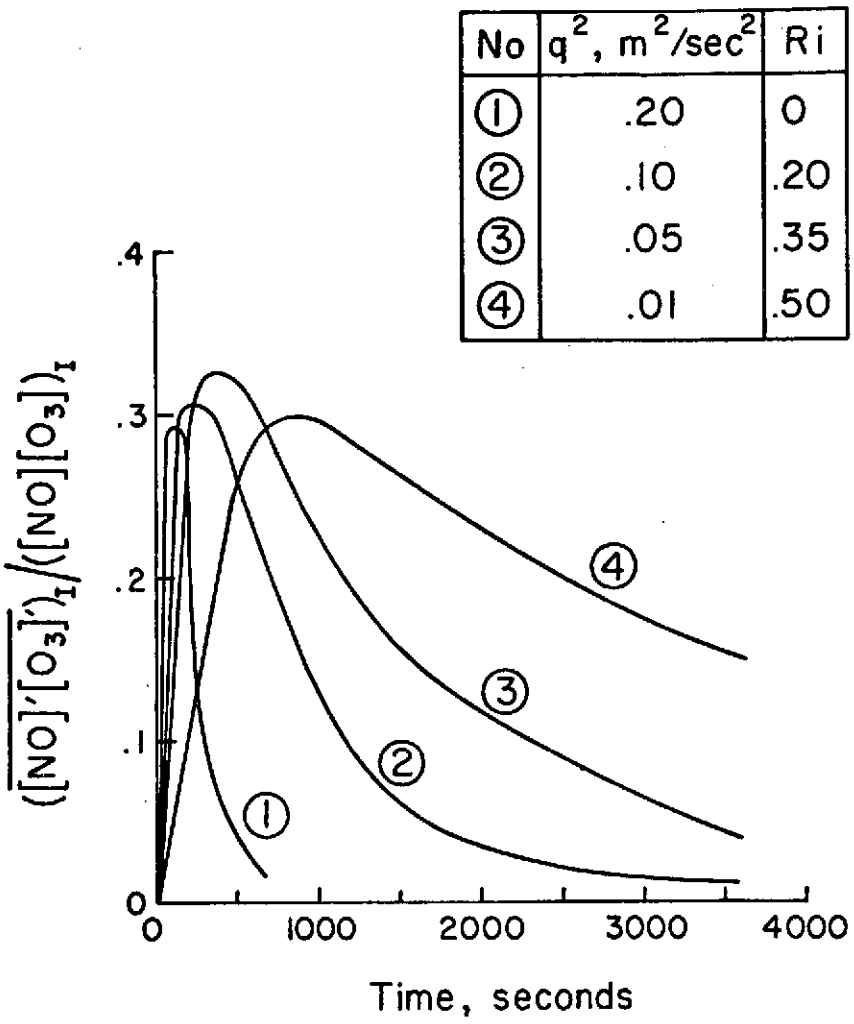

Figure A1. Time history of the mixedness, integrated over the plume width, as a function of turbulence and stability.

REFERENCES

1. Donaldson, C. duP.: Construction of a Dynamic Model of the Production of Atmospheric Turbulence and the Dispersal of Atmospheric Pollutants. Workshop on Micrometeorology, (D. A. Haugen, ed.), American Meteorological Society, Science Press, Ephrata, Pa., pp. 313-390, 1973.

2. Hilst, G. R., et al.: The Development and Preliminary Application of an Invariant Coupled Diffusion and Chemistry Model. NASA CR-2295, 1973.

3. Waco, D. E.: Stratospheric Mixing Estimated from High Altitude Turbulence Measurements. J. Appl. Meteor. (in press), 1974.

4. Hilst, G. R., and Donaldson, C. duP.: Preliminary Estimates of the the Fate of SST Exhaust Materials Using a Coupled Diffusion/ Chemistry Model. AIAA Paper No. 73-535, Denver, Colo., 1973.

5. Hilst, G. R. et al.: Some Analyses of the Chemistry and Diffusion of SST Exhaust Materials During Phase III of the Wake Period. Proceedings of IAMAP First Special Assembly (UAPRC), Melbourne (in press), 1974.

6. Donaldson, C. duP.: A Computer Study of an Analytical Model of Boundary Layer Transition. AIAA J. Vol. 7, No. 2, pp. 272-278, 1969.

7. Donaldson, C. duP., and Sullivan R. D.: Decay of an Isolated Vortex. Aircraft Wake Turbulence and Its Detection, (J. Olsen, A. Goldburg, M. Rogers, eds.), Plenum Press, NYC, pp. 389-411, 1971.

8. Donaldson, C. duP. and Hilst, G. R.: Effect of Inhomogeneous Mixing on Atmospheric Photochemical Reactions. Env. Sci. and Tech., Vol. 6, pp. 812-816, 1972.

9. Hilst, G. R. and Contiliano, R.: A Preliminary Sensitivity Analysis of the Coupled Diffusion and Chemistry Model. NASA CR-132369, 65 pp., 1973.

10. Keller, L. V. and Friedman, A. A.: Differential-Gleichung für die Turbulente Bewegung Einer Kompressiblen Flüssigkeit. Proceedings 1st Intern. Cong. Appl. Mech., Delft, 1924.

11. Reynolds, O.: On the Dynamical Theory of Incompressible Viscous Fluids and the Determination of the Criterion. Phil. Trans. Roy. Soc., London, pp. 123-161, 1894.

12. Johnston, H. S.: Reduction of Stratospheric Ozone by Nitrogen Oxide Catalysts from Supersonic Transport Exhaust. Science, Vol. 173, pp. 517-522, 1971.

13. Garvin, D., et al.(eds.): Chemical Kinetics Data Survey. NBSIR 74-430, Phys. Chem. Div., NBS, Washington, D. C., 1973.

14. Crutzen, P. J.: Ozone Production Rates in an Oxygen-Hydrogen-Nitrogen Oxide Atmosphere. J. Geophys. Res., Vol. 76, p. 7315, 1971.

15. Hoshisaki, H.: Aircraft Wake Micro-Scale Phenomenon. CIAP Report 3, pp. 2-3, 1973.

16. Galinas, R.: Kinetic Models. CIAP Report 3, pp. 4-45, 1973.

17. Walton, J. J.: Dispersion of SST Exhaust Plumes in the Stratosphere. Proceedings of IAMAP First Special Assembly (UAPRC), Melbourne (in press), 1974.

18. Gudiksen, P. H., et al.: Roles of Mean Meridional Circulation and Eddy Diffusion in the Transport of Trace Substance in the Lower Stratosphere. J. Geophys. Res., Vol. 73, pp. 4461-4473, 1968.

19. Forney, K.: Private Communication, 1974.